STABILITY AND COEXISTENCE IN LARGE ECOLOGICAL SYSTEMS

M.Sc Thesis

By

Suman Birda



STABILITY AND COEXISTENCE IN LARGE ECOLOGICAL SYSTEMS

A THESIS

Submitted in partial fulfillment of the requirements for the award of the degree

of

MASTERS OF SCIENCE

by

Suman Birda



CANDIDATE'S DECLARATION

I hereby certify that the work which is being presented in this thesis entitled "STA-BILITY AND COEXISTENCE IN LARGE ECOLOGICAL SYSTEMS" in the partial fulfillment of the requirements for the award of the degree of MASTER OF SCIENCE and submitted in the DEPARTMENT OF PHYSICS, Indian Institute Of Technology Indore, is an authentic record of my own work carried out during the time period from May 2024 to May 2025 under the supervision of Dr. Deepak Gupta (thesis supervisor) and Dr. Mritunjay Kumar Verma, Assistant Professor, Department of Physics, Indian Institute of Technology Indore.

The matter presented in this thesis has not been submitted by me for the award of any other degrees of this or any other institute.

| | Suman Bisda Suman Birda |
|---|----------------------------------|
| | |
| This is to certify that the above statement made by the | candidate is correct to the best |
| of my knowledge. | Departa |
| | Dr. Deepak Gupta |
| | |

viitingy Kung

Dipankar Das

DPGC Signature

| | | | | | | | | | | | | | | Г | r | • | N | Ir | it | u | n | ja | y | ŀ | ζı | ur | na | ar | V | eı | m | ıa |
|--|--|--|--|--|--|--|--|--|--|--|--|--|--|---|---|---|---|----|----|---|---|----|---|---|----|----|----|----|---|----|---|----|
| | | | | | | | | | | | | | | | | | | | | | | | | | | | | | | | | |
| | | | | | | | | | | | | | | | | | | | | | | | | | | | | | | | | |

Suman Birda, has successfully given his M.Sc. Oral examination held on 13/5/2025

Thesis supervisor Signature

Dr. Deepak Gupta

Date: 20/5/2025 Date: 20/5/2025

Multinguy Kumay Administrative supervisor Signature

Dr. Mritunjay Kumar Verma

Date: 20/5/2025

ACKNOWLEDGEMENT

I would like to express my deepest gratitude to my thesis supervisor, Dr. Deepak Gupta, for his invaluable guidance throughout my project. His continuous support, insightful advice, and encouragement have played a crucial role in shaping my understanding and growth as a researcher. He has taught me many new concepts and always motivated me to strive for excellence in my work.

I am also grateful to my supervisor, Dr. Mritunjay Kumar Verma, who, although not directly involved in guiding my project, was always available whenever I needed his support. His presence during important moments such as presentations and institutional matters provided me with the necessary confidence and assistance.

Finally, I extend my heartfelt thanks to my friends and my parents, whose unwavering emotional support has been a source of strength throughout this journey. Their encouragement and belief in me have been invaluable during this time.

ABSTRACT

Understanding the conditions that govern the stability and coexistence of species in ecological systems remains a central challenge in theoretical ecology. In this thesis, we explore this problem through three distinct but complementary approaches grounded in random matrix theory and consumer-resource dynamics.

We begin by revisiting May's stability criterion for large random ecosystems and extend it using the Circular Law. By incorporating sparsity and variance scaling, we derive analytical stability conditions and validate them through numerical simulations. Next, we revisit the competitive exclusion principle within the framework of consumer-resource models, demonstrating how resource availability and half-saturation constants (which quantify the resource level at which a species achieves half its maximum growth rate) govern species persistence and extinction. Finally, we investigate how asymmetric migration between habitats can promote coexistence beyond classical resource-based constraints. We derive conditions for stable stationary states and analyze how effective competition coefficients shape biodiversity outcomes.

Together, these investigations offer insights into the spectral and ecological mechanisms that underpin the stability and diversity of complex ecosystems.

Contents

| 1 | Intr | roduction | 1 | | | | | | | |
|---|------|--|----|--|--|--|--|--|--|--|
| 2 | Stal | Stability of Random Ecosystem | | | | | | | | |
| | 2.1 | Introduction | 5 | | | | | | | |
| | 2.2 | Random variable | 7 | | | | | | | |
| | | 2.2.1 Types of random variables | 8 | | | | | | | |
| | 2.3 | Probability distribution and related functions | 8 | | | | | | | |
| | | 2.3.1 Probability distribution | 8 | | | | | | | |
| | | 2.3.2 Probability Mass Function (PMF) | 9 | | | | | | | |
| | | 2.3.3 Probability Density Function (PDF) | 10 | | | | | | | |
| | | 2.3.4 Cumulative Distribution Function (CDF) | 11 | | | | | | | |
| | 2.4 | Normal distribution or Gaussian distribution | 12 | | | | | | | |

| | 2.5 | Uniform distribution | 13 |
|---|------|---|----|
| | 2.6 | Exponential distribution | 14 |
| | 2.7 | Log-Normal distribution | 15 |
| | 2.8 | Random matrix | 16 |
| | | 2.8.1 Types of random matrices | 16 |
| | 2.9 | Circular Law | 21 |
| | 2.10 | Stability Analysis and the Circular Law | 21 |
| | | 2.10.1 Circular Law Discussion | 21 |
| | | 2.10.2 Stability Criteria | 23 |
| | 2.11 | Conclusion | 32 |
| 3 | Con | npetitive exclusion principle | 34 |
| | 3.1 | Introduction | 34 |
| | 3.2 | Consumer-Resource Model | 35 |
| | 3.3 | Competition for a single resource | 37 |
| | | 3.3.1 One species and one resource | 38 |
| | | 3.3.2 Two species and one resource | 39 |
| | 3.4 | Competition for two resources | 43 |

| | | 3.4.1 | Two resources and one species | 45 |
|---|-----|---------|--|----|
| | | 3.4.2 | Two resources and two species | 47 |
| | 3.5 | Conclu | asion | 55 |
| 4 | Spe | cies Co | pexistence via Asymmetric Migration | 57 |
| | 4.1 | Introd | uction | 57 |
| | 4.2 | Asymr | metric Migration Model | 58 |
| | 4.3 | Effecti | ve Asymmetric Migration model | 61 |
| | 4.4 | Specie | s coexistence: Stationary state and stability analysis | 64 |
| | | 4.4.1 | Stationary states of the system | 64 |
| | | 4.4.2 | Stability analysis | 66 |
| | | 4.4.3 | Coexistence condition in terms of original competition coefficients $(\alpha_{12} \text{ and } \alpha_{21}) \ldots \ldots \ldots \ldots \ldots \ldots$ | 73 |
| | 4.5 | Conclu | asion | 75 |
| 5 | Sun | nmary | and outlook | 77 |
| 6 | AP | PEND | IX | 81 |
| | 6.1 | Euler's | s Method | 81 |
| | | 611 | Error Analysis in Euler's Method | 85 |

Chapter 1

Introduction

Nature is a dynamic system of remarkable diversity and complexity. From lush rainforests to microscopic communities in a drop of water, ecosystems sustain life through intricate networks of interactions among species and their environments. Yet, these systems are fragile — they can shift dramatically or collapse when disturbed by climate change, habitat fragmentation, species invasions, or other perturbations. A central question in ecology and sustainability science therefore emerges: What makes an ecosystem stable? And under what conditions can many species coexist despite competition for limited resources?

This question becomes even more critical today, as biodiversity declines and human impacts intensify. Understanding how and when species-rich communities persist is not only a theoretical challenge but a practical necessity — one that underpins conservation, food security, and climate resilience strategies worldwide [1, 2, 3].

Theoretical ecologists have long pursued this question using mathematical models.

Classic work by Lotka [4] and Volterra [5] introduced deterministic differential equations to capture predator-prey and competitive interactions. While these models offer foundational insights, they typically consider only a few species and often assume equilibrium conditions. Real ecosystems, by contrast, involve hundreds or thousands of species, non-linear interactions, spatial heterogeneity, and stochastic events [6, 7].

A paradigm shift occurred in 1972 with the work of Robert May, who asked whether complexity begets stability or undermines it. Using random matrix theory (RMT), May modeled the interaction matrix of species in an ecosystem as a large random matrix and showed that beyond a critical threshold of interaction strength or network complexity, the system becomes unstable [8, 9]. His now-famous result — that stability requires $\sigma \sqrt{NC} < 1$, where σ is the standard deviation of interaction strength, N the number of species, and C the connectance—challenged the prevailing intuition that biodiversity guarantees resilience.

This result spurred decades of research. Ecologists, physicists, and mathematicians extended May's ideas, exploring the spectral properties of random matrices and applying tools like the Circular Law, which describes how eigenvalues of large random matrices with independent and identically distributed entries are uniformly distributed in a disk of radius $\sigma\sqrt{NC}$ in the complex plane [10]. Allesina and Tang [11] further adapted these models to biological realism by distinguishing between mutualistic, competitive, and trophic interactions. Extensions have also explored the effects of empirical network structures, modularity, and correlation patterns on stability [12, 13, 14]. These spectral approaches provide statistical predictions for the probability that a random ecosystem is stable — a "null model" baseline against which real ecological networks can be compared.

However, such global or "top-down" models have limitations. They lack mechanis-

tic specificity: they tell us whether random interactions could be stable, but not why a particular set of species does or does not coexist. To address this, bottom-up approaches revisit the classical competitive exclusion principle (CEP) — the idea that no two species can coexist if they compete for the exact same limiting resource under fixed environmental conditions [15, 16].

Using the consumer-resource framework originally developed by MacArthur [17] and later extended by Tilman [18], researchers analyze how species traits, resource availability, and consumption strategies determine whether coexistence or exclusion occurs. Geometric tools like Zero Net Growth Isoclines (ZNGIs) provide intuitive and visual insights into these dynamics. These models highlight the importance of niche differentiation and trade-offs in promoting biodiversity [19, 17].

Yet, in nature, coexistence often arises under conditions that seem to contradict classical theory. One key reason is spatial structure. Species inhabit patchy landscapes and often migrate between habitats. Migration creates spatial refuges, alters effective interactions, and allows species to persist even when local competition would drive them extinct. Asymmetric migration, in which movement rates differ between species or directions, can play a crucial role in shaping regional coexistence. This spatial dimension brings ecological modeling closer to real-world dynamics, linking local interaction rules to landscape-level persistence [20, 21].

In this thesis, we develop and analyze models that explore how structural complexity, resource competition, and migration interact to determine the stability and coexistence of ecological communities. Our work integrates random matrix theory, consumer-resource dynamics, and spatial modeling to gain new insights into when biodiversity is maintained or lost in competitive ecosystems.

Chapter 2

Stability of Random Ecosystem

2.1 Introduction

In the previous chapter, we outlined the central ecological challenge of understanding the conditions under which species coexist and ecosystems remain stable. One influential approach to this problem was developed by Robert May, who applied random matrix theory to study the stability of large ecological networks [8]. His work showed that increasing complexity — in terms of the number of species, the strength of their interactions, and the density of connections — can lead to a loss of stability, contrary to earlier ecological intuition [22, 23].

This chapter presents a theoretical and computational investigation of how the structure and strength of species interactions influence ecosystem stability. Here, stability refers to whether the system returns to its equilibrium after a small disturbance — a condition determined by the eigenvalues of the community matrix.

To ground this abstract idea in an ecological context, consider the following story:

Imagine a dense forest full of life — towering trees, chirping birds, buzzing insects, hidden fungi, and stealthy predators. Each species plays a role in a vast web of interactions: pollination, predation, decomposition, and competition. Now, imagine a sudden disruption: a fungal disease wipes out one of the dominant tree species, a keystone that many others relied on for food, shelter, or structure. What happens next depends on the forest's ability to adapt.

In one forest, the system manages to absorb the shock. Birds find new trees to nest in. Herbivores adjust their diets. Over time, other tree species spread into the open space. The web of interactions rearranges itself, and the ecosystem settles into a new, stable state.

In another forest, however, the same loss sets off a chain reaction. Insects that depended on the dead tree vanish. Birds that relied on those insects for food or the tree for nesting space disappear. Predators lose their prey. One disruption leads to another, and the ecosystem begins to collapse.

What makes the difference? Stability is not just about the number or diversity of species, but about how they interact and how these interactions are structured.

May's framework offers a way to study such questions mathematically, treating the ecosystem as a network and analyzing its stability through the lens of linear dynamics and random matrices. May's theory allows us to ask whether such resilience can be predicted just from the structure of the interaction network — without needing to model every species in detail.

In this chapter, we revisit and extend this framework. We analyze how features such as sparsity in the interaction matrix [11], variance scaling [12], and nontrivial eigenvalue distributions [24] modify the classical Circular Law [25, 26] and affect the conditions for local stability.

To do this, we begin by introducing the key mathematical background, including random variables, probability distributions, and the construction of random matrices. We then define the community matrix and describe how its eigenvalues relate to local stability. Using numerical simulations, we verify theoretical predictions and examine how increasing complexity and structural properties influence the resilience of large ecosystems.

This approach not only deepens our understanding of when complex ecosystems can remain stable, but also provides a benchmark—a null model—against which more structured, biologically realistic systems can be compared [27, 28].

2.2 Random variable

A random variable represents a quantity that can attain different values, with each value occurring based on a certain probability. The outcome is determined by a random process.

2.2.1 Types of random variables

Discrete random variables

A discrete random variable can only take specific, separate values. These values are usually countable, such as the number of customers arriving at a small café in an hour. Let Z represent this number. The café might receive 0, 1, 2, 3, ... customers, but it cannot receive a fractional number of customers (like 2.5).

Continuous random variables

A continuous random variable can attain any value within a defined range. These values are not limited to distinct numbers but instead span a continuum. For example, a person's age can be measured to arbitrary precision within a certain range.

2.3 Probability distribution and related functions

2.3.1 Probability distribution

A probability distribution defines how the probability of a random variable is spread across its possible values. It describes the chances of different outcomes occurring in a given situation. Depending on the type of random variable, a probability distribution can be either discrete, where the values are distinct, or continuous, where the values form an uninterrupted range.

Discrete probability distribution

A discrete probability distribution applies when a random variable can assume a specific set of separate, countable values. For instance, the number of times a bus arrives at a stop within an hour follows a discrete probability distribution, as the count can only be whole numbers like 0, 1, 2, and so on.

Continuous probability distribution

A continuous probability distribution represents situations where a random variable can take endlessly many values within a certain range. For example, the time a runner takes to finish a race follows a continuous probability distribution, since it can be measured with infinite precision within a given interval.

2.3.2 Probability Mass Function (PMF)

The probability mass function characterizes the likelihood distribution of a discrete random variable by assigning a probability to each specific outcome it can attain. A fundamental property of the PMF is that the cumulative sum of these probabilities across all conceivable values of the random variable must be exactly 1. For example: Suppose a robotic sensor detects objects moving past a checkpoint and registers the count per minute. If the sensor can detect up to five objects in a given minute with equal probability, then the probability mass function is:

$$P(Z = z_i) = \frac{1}{5}$$
, for $z_i \in \{1, 2, 3, 4, 5\}$. (2.1)

2.3.3 Probability Density Function (PDF)

A probability density function characterizes how a continuous random variable distributes its likelihood over an interval of possible values. Unlike discrete cases where individual outcomes hold specific probabilities, a PDF instead describes the tendency of the variable to manifest within a given range. The probability of the variable assuming a value between two points, say a and b, is obtained by computing the integral of the PDF over that interval:

$$P(a \le Z \le b) = \int_{a}^{b} f_{Z}(z) dz$$
 (2.2)

Since the continuous variable can take infinitely many values, the total accumulation of probabilities over all possible outcomes—represented by the area under the PDF curve—must sum to exactly one.

To illustrate, consider an autonomous vehicle equipped with a sensor that measures the precise reaction time of its braking system, recorded in seconds. If the reaction time Z is uniformly distributed between 2 and 4 seconds, the corresponding PDF is:

$$f_Z(z) = \begin{cases} \frac{1}{2}, & 2 \le z \le 4, \\ 0, & \text{otherwise}. \end{cases}$$
 (2.3)

If we wish to determine the probability that the braking reaction time falls between 2.5 and 3.2 seconds, we integrate the PDF over this interval:

$$P(2.5 \le Z \le 3.2) = \int_{2.5}^{3.2} \frac{1}{2} dz = \frac{3.2 - 2.5}{2} = 0.35$$
 (2.4)

This example highlights how a PDF provides insight into the behavior of continuously varying phenomena, where probabilities are associated with ranges rather than distinct values.

2.3.4 Cumulative Distribution Function (CDF)

The cumulative distribution function quantifies the probability that a random variable Z assumes a value no greater than a given threshold z. Unlike probability mass and density functions, which describe probabilities at specific points, the CDF provides a cumulative perspective, capturing the aggregated probability up to a certain value. This formulation is applicable to both discrete and continuous variables.

For a discrete random variable, the CDF is obtained by summing the probabilities of all possible values up to z:

$$F_Z(z) = P(Z \le z) = \sum_{z_i \le z} P(Z = z_i)$$
 (2.5)

Consider an intelligent lighting system in a building that randomly activates between 1 and 5 ceiling lights at any given time. If the system distributes this activation uniformly, the probability of having up to 3 lights turned on at a particular moment is given by:

$$F_Z(3) = P(Z \le 3) = P(Z = 1) + P(Z = 2) + P(Z = 3) = \frac{3}{5}$$
 (2.6)

For a continuous random variable, the CDF is computed by integrating the probability density function from negative infinity up to z:

$$F_Z(z) = P(Z \le z) = \int_{-\infty}^z f_Z(z) dz$$
 (2.7)

As an example, suppose an automated coffee machine dispenses liquid volumes between 150 ml and 250 ml in a uniformly random manner. The corresponding CDF is:

$$F_Z(z) = \begin{cases} 0 , & z < 150 ,\\ \frac{z - 150}{100} , & 150 \le z \le 250 ,\\ 1 , & z > 250 . \end{cases}$$
 (2.8)

This implies that the probability of receiving a volume of coffee no greater than z increases linearly between 150 ml and 250 ml, starting at zero and reaching certainty at the upper bound.

2.4 Normal distribution or Gaussian distribution

The normal distribution is a fundamental concept in probability theory, describing how values of a continuous random variable are symmetrically dispersed around a central location. This distribution naturally emerges in numerous real-world scenarios due to the Central Limit Theorem, which states that the sum of independent and identically distributed random variables typically has a normal distribution. Its PDF is given by:

$$f_Z(z) = \frac{1}{\sqrt{2\pi\sigma^2}} e^{-\frac{(z-\mu)^2}{2\sigma^2}}, \quad z \in \mathbb{R} .$$
 (2.9)

Here, μ signifies the average or expected value of the distribution, while σ quantifies the extent of dispersion around the mean, determining how widely the values fluctuate.

A compelling example of this distribution appears in precision manufacturing. Suppose a factory produces high-precision metal rods, each intended to be exactly 10 cm in length. However, due to microscopic variations in the manufacturing process, the actual lengths deviate slightly from this ideal value. When measured, the lengths of these rods cluster around 10 cm, with minor variations symmetrically distributed on either side—forming a normal distribution. This pattern allows engineers to quantify production consistency, identify defects, and optimize the process to minimize deviations.

2.5 Uniform distribution

The uniform distribution describes a probability distribution where every outcome in a given range is equally probable. Its probability density function remains constant within a specified interval [c, d] and is given by:

$$f_Z(z) = \frac{1}{d-c}, \quad \text{for } c \le z \le d \ . \tag{2.10}$$

In this distribution, the values c and d define the lower and upper limits, respectively. A practical illustration of this distribution can be found in automated packaging systems. Imagine a robotic arm that randomly places identical items into boxes within a designated area. If the robot is programmed to position objects uniformly across a conveyor

belt spanning from position c to position d, then the likelihood of an item being placed at any specific point in this range is constant. This uniform probability distribution enables optimized loading strategies and efficient space utilization.

2.6 Exponential distribution

The exponential distribution characterizes the likelihood of waiting times between occurrences of randomly occurring events that are independent and follow a constant average rate. It is particularly relevant in scenarios where the timing of the next event depends only on the present moment and not on past occurrences. Its probability density function (PDF) is given by:

$$f_Z(z) = \lambda e^{-\lambda z} , \quad z \ge 0 , \qquad (2.11)$$

where λ is a positive rate parameter that signifies how frequently events take place per unit time.

A distinctive example of this distribution can be found in the context of self-checkout stations at supermarkets. Imagine a system where customers arrive at random, and each person takes an unpredictable amount of time to complete their transaction. The duration between successive checkouts follows an exponential distribution, as each customer's speed is independent of the previous one. Understanding this pattern helps store managers optimize the number of machines required to minimize congestion while maintaining efficiency.

2.7 Log-Normal distribution

The log-normal distribution describes a scenario where the logarithm of a random variable exhibits a normal distribution. In other words, if a variable Z follows a log-normal distribution, then $\ln(Z)$ conforms to a normal distribution. This distribution is particularly valuable when analyzing data that grow multiplicatively or display a right-skewed pattern. The probability density function (PDF) of a log-normal distribution is given by:

$$f_Z(z) = \frac{1}{z\sigma\sqrt{2\pi}}e^{-\frac{(\ln(z)-\mu)^2}{2\sigma^2}}, \quad z > 0 ,$$
 (2.12)

where μ and σ represent the mean and standard deviation of $\ln(Z)$, respectively.

A unique example of this distribution emerges in the analysis of technological innovation lifespans. Consider the time it takes for a newly introduced product, such as a smartphone model, to reach peak adoption and subsequently decline in usage. Unlike a normal distribution, where deviations are symmetric around the mean, technological adoption rates often experience a rapid rise followed by a slower decline—closely resembling a log-normal pattern. Understanding this distribution helps companies predict the longevity of innovations and optimize product life cycles.

So far, we have focused on various probability distributions to model the behavior of individual random variables. However, many systems of interest involve a large number of interacting components, where randomness appears not in isolation but collectively. In such cases, instead of studying scalar random variables, we consider matrices whose entries are drawn from these distributions. This shift allows us to capture the complexity

of high-dimensional systems, and leads us to the framework of random matrix theory—where the properties of large matrices with random entries reveal deep insights about stability, dynamics, and structure.

2.8 Random matrix

In a random matrix, some or all of its elements are random variables (Sec. 2.2), meaning their values are determined according to specified probability distributions (Secs. 2.4, 2.5, 2.6, and 2.7). Random matrices are used to model complex systems where uncertainty or randomness plays a central role. Their analysis often focuses on statistical properties such as the distribution of eigenvalues, singular values, or the behavior of entries as the matrix size grows.

2.8.1 Types of random matrices

Random matrices are classified based on the distributions of their entries and structural properties. Below, we describe several common types of random matrices, their definitions, and examples.

Gaussian random matrix

A matrix where all entries are independently drawn from a Gaussian (normal) distribution, typically with mean μ and variance σ^2 [29]. The entries are real-valued, $A_{ij} \sim \mathcal{N}(\mu, \sigma^2)$. For example: A 3 × 3 Gaussian random matrix with $\mu = 0$ and

$$\sigma^2 = 1:$$

$$A = \begin{bmatrix} 0.31 & -1.44 & 0.79 \\ -0.54 & 0.93 & 1.01 \\ -1.22 & 0.43 & -0.67 \end{bmatrix}.$$

This type of matrix is commonly used in signal processing, machine learning, and modeling physical systems due to the well-understood statistical behavior of Gaussian distributions.

Wigner random matrix

A symmetric matrix where the diagonal entries are real-valued random variables, and the off-diagonal entries are independent and identically distributed random variables [30]. The matrix satisfies $A_{ij} = A_{ji}$, and typically the diagonal entries are also drawn from a normal distribution. Specifically, $A_{ii} \sim \mathcal{N}(0,1)$ and $A_{ij} \sim \mathcal{N}(0,1)$ for $i \neq j$. For example: A 3 × 3 Wigner matrix with off-diagonal entries $A_{ij} \sim \mathcal{N}(0,1)$:

$$A = \begin{bmatrix} 1.21 & -0.65 & 0.45 \\ -0.87 & 0.58 & 1.01 \\ 0.65 & 1.03 & -1.11 \end{bmatrix} . \tag{2.14}$$

(2.13)

Wigner matrices are central to spectral analysis and are widely applied in nuclear physics and the study of random graphs.

Wishart random matrix

A positive semi-definite matrix obtained by multiplying a data matrix X (with random entries) by its transpose: $W = X^{\top}X$ [31]. If the entries of X are drawn from a multivariate normal distribution, then the resulting matrix W follows a Wishart distribution. Specifically, for $X \sim \mathcal{N}(0, \Sigma)$, the matrix W is a Wishart matrix.

However, if the entries of X are drawn from a distribution other than the normal distribution, the resulting matrix $W = X^{\top}X$ will not follow a Wishart distribution, but it may still have properties relevant for specific applications, depending on the chosen distribution. For example: Let X be a 3×2 matrix with $X_{ij} \sim \mathcal{N}(0, 1)$:

$$X = \begin{bmatrix} 1.2 & -0.5 \\ 0.7 & 1.3 \\ -0.4 & 0.8 \end{bmatrix} . \tag{2.15}$$

The Wishart matrix is $W = X^{\top}X$:

$$W = \begin{bmatrix} 2.13 & -0.41 \\ -0.41 & 2.38 \end{bmatrix} . \tag{2.16}$$

Wishart matrices play a key role in covariance estimation, multivariate statistics, and financial modeling, where understanding the structure of variability is essential.

Uniform random matrix

A matrix where each entry is independently drawn from a uniform distribution over an interval [c, d] [32]. The entries are real-valued, $A_{ij} \sim \text{Uniform}(a, b)$. For example: A

 2×2 uniform random matrix with entries drawn from [0, 1]:

$$A = \begin{bmatrix} 0.31 & 0.86 \\ 0.43 & 0.24 \end{bmatrix} . \tag{2.17}$$

Uniform random matrices are frequently used in Monte Carlo simulations and certain machine learning applications where uniformly distributed randomness is desired.

Exponential random matrix

A matrix where each entry is independently drawn from an exponential distribution with rate parameter $\lambda > 0$ [33]. The entries are real-valued, $A_{ij} \sim \text{Exponential}(\lambda)$. For example: A 2 × 2 exponential random matrix with $\lambda = 2$:

$$A = \begin{bmatrix} 0.23 & 0.78 \\ 0.45 & 0.12 \end{bmatrix} . \tag{2.18}$$

These matrices find applications in reliability engineering, queuing theory, and stochastic modeling where waiting times or decay processes are modeled.

Sparse random matrix

A matrix where most of the entries are 0, and nonzero entries are random variables, often drawn from a specific distribution [34]. The sparsity is controlled by a parameter p, which represents the fraction of non-zero elements in the matrix. For example: A 4×4

sparse random matrix with sparsity p = 0.25, and nonzero entries $A_{ij} \sim \mathcal{N}(0, 1)$:

$$A = \begin{bmatrix} 0 & 0 & -0.45 & 0 \\ 0 & 0.67 & 0 & 0 \\ 0 & 0 & 0 & -1.23 \\ 0.89 & 0 & 0 & 0 \end{bmatrix} . \tag{2.19}$$

Sparse random matrices are essential in network analysis and modeling large-scale systems, particularly when only a small fraction of interactions or connections are active.

Log-Normal random matrix

A matrix where each entry is independently drawn from a log-normal distribution. The logarithm of the entries follows a normal distribution: $A_{ij} \sim \text{LogNormal}(\mu, \sigma^2)$ [35]. For example: A 2 × 2 log-normal random matrix with $\mu = 0$ and $\sigma = 1$:

$$A = \begin{bmatrix} 1.75 & 3.22 \\ 0.85 & 4.56 \end{bmatrix} . \tag{2.20}$$

Log-normal matrices are useful in modeling financial returns and multiplicative growth processes, where the logarithm of the variable of interest is normally distributed.

Having introduced various types of random matrices and their applications, we now turn to one of the central results in random matrix theory—the circular law. This law characterizes the asymptotic distribution of eigenvalues for large non-Hermitian random matrices with independent, identically distributed entries. Understanding this result is crucial for analyzing the stability of complex systems, where the eigenvalue spectrum determines the response to perturbations.

2.9 Circular Law

2.10 Stability Analysis and the Circular Law

In dynamical systems analysis, assessing stability fundamentally revolves around scrutinizing the eigenvalues of the system's Jacobian matrix. Stability is established when every eigenvalue of this matrix possesses a real part that is strictly negative, ensuring perturbations diminish over time rather than amplify [36].

A fascinating insight from random matrix theory, known as the Circular Law [26], characterizes the spectral behavior of large random matrices whose elements are independently drawn from identical probability distributions. This law reveals that as the matrix dimension grows, its eigenvalues asymptotically scatter within a circular region in the complex plane, offering profound implications for understanding stability in high-dimensional, complex systems.

2.10.1 Circular Law Discussion

May's analysis of ecosystem stability leads to the consideration of random matrices in determining system behavior. The stability of a large ecological community can be studied using the eigenvalues of the interaction matrix M, which is drawn from a distribution with mean zero and variance σ^2 . A key result in random matrix theory is the circular

law, which states that as the matrix size grows $(N \to \infty)$, the eigenvalues of M become uniformly distributed within a circle of radius $\sigma \sqrt{N}$ in the complex plane [26, 25].

Specifically, consider a system with N variables (in an ecological application these are the populations of the N interacting species) which in general may obey some quite non-linear set of first-order differential equations. The stability of the possible equilibrium or time-independent configurations of such a system may be studied by Taylor-expanding in the neighborhood of the equilibrium point, so that the stability of the possible equilibrium is characterized by the equation:

$$\frac{dx}{dt} = Mx \ . {(2.21)}$$

Here, in an ecological context, x is the $N \times 1$ column vector of the disturbed populations x_i , and the $N \times N$ interaction matrix M has elements M_{ik} which characterize the effect of species k on species i near equilibrium. The structure of M reflects the underlying ecological interactions: an entry M_{ik} is zero if species k does not directly affect species i, and its sign and magnitude encode the nature and strength of the interaction. For example, mutualistic, competitive, or predator-prey relationships correspond to different combinations of signs and magnitudes in M.

To understand the dynamics of species populations in such systems, we consider Eq. (2.21). The stability of the system depends on whether the real parts of the eigenvalues of M are negative; if at least one eigenvalue has a positive real part, the system is unstable.

This formulation provides a direct connection between May's stability criterion and the spectral properties of random matrices, highlighting the importance of eigenvalue distributions in ecological and complex system dynamics. A natural extension of this idea is to analyze how the eigenvalue distribution of a random matrix changes under different assumptions about its entries. This leads to a more general formulation of the circular law, which helps refine our understanding of stability conditions in large systems.

2.10.2 Stability Criteria

The "circular law" states that for a large $N \times N$ matrix M, whose entries (both diagonal and off-diagonal) are independently drawn from a distribution with mean 0 and variance 1, the eigenvalues of M become uniformly distributed within a circle in the complex plane as $N \to \infty$ (see Figs. 2.1 and 2.2). This result is crucial in understanding the spectral properties of large random matrices. The radius of this circle, centered at the origin (0,0), is given by:

$$R = \sqrt{N} \ . \tag{2.22}$$

To normalize the eigenvalues and ensure a scale-independent analysis, we consider the matrix M/\sqrt{N} . Plotting its eigenvalues reveals a circular distribution centered at the origin with a unit radius.

Extending the Circular Law with Rescaling

Now, consider another matrix M' of size $N \times N$, where all elements are drawn from a distribution with zero mean and variance σ^2 . By rescaling, we define:

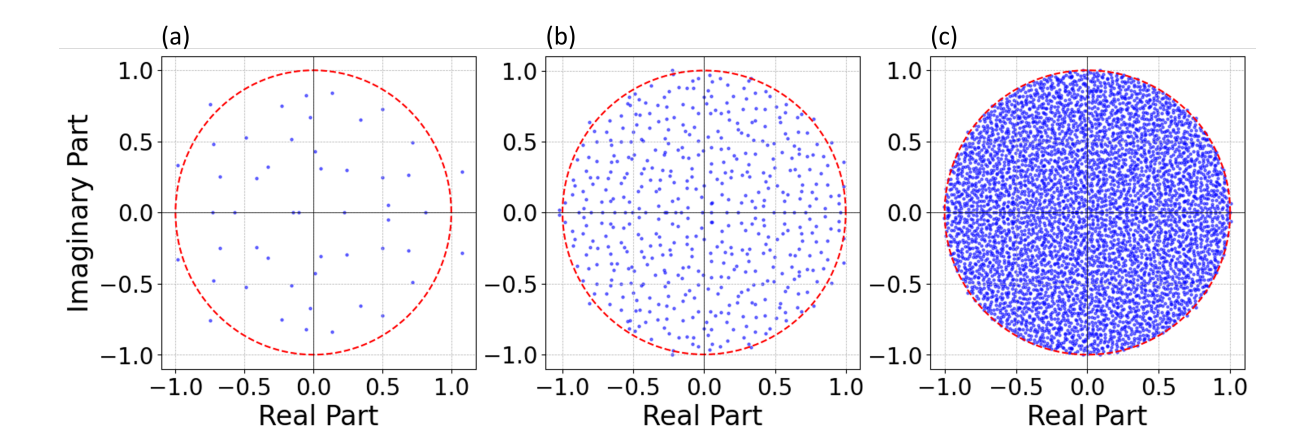


Figure 2.1: Eigenvalue distribution of random matrices whose elements are independently sampled from a normal distribution with variance 1 and mean 0. Panels (a), (b), and (c) correspond to N = 50, N = 500, and N = 5000, respectively. Eigenvalues (blue dots) are plotted in the complex plane after rescaling by \sqrt{N} . The red dashed line represents the unit circle.

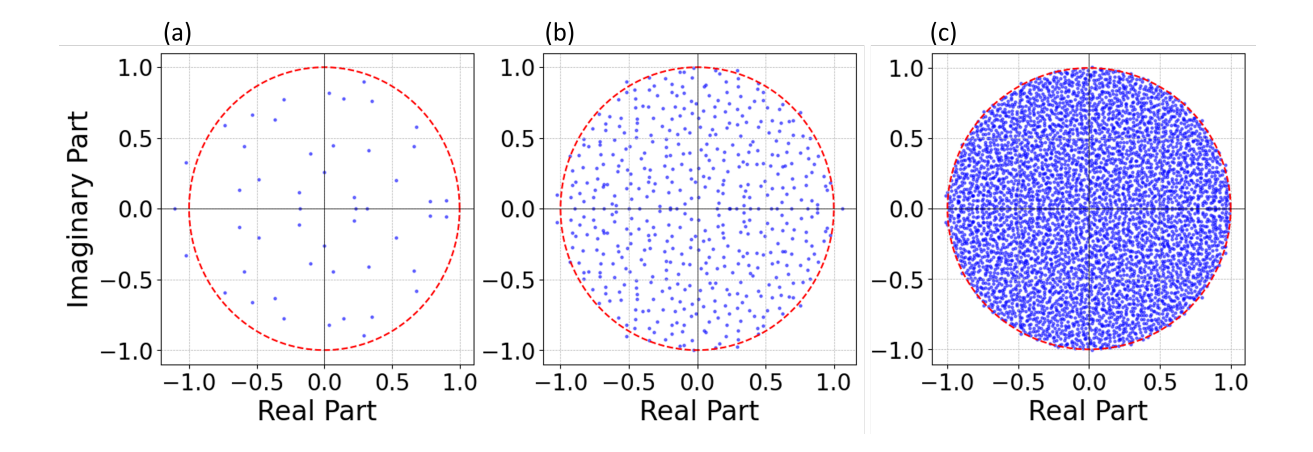


Figure 2.2: Eigenvalue distribution of random matrices whose elements are independently sampled from a uniform distribution with variance 1 and mean 0. Panels (a), (b), and (c) correspond to N = 50, N = 500, and N = 5000, respectively. Eigenvalues (blue dots) are plotted in the complex plane after rescaling by \sqrt{N} . The red dashed line represents the unit circle.

$$M = \frac{1}{\sigma}M' \,, \tag{2.23}$$

which ensures that M has zero mean and unit variance. Consequently, normalizing by \sqrt{N} gives:

$$\frac{M}{\sqrt{N}} = \frac{1}{\sqrt{N}\sigma}M' \,\,\,\,(2.24)$$

where each side retains a unit radius and is centered at the origin. This step illustrates how variance scaling affects the eigenvalue distribution.

Introducing Probability-Dependent Sparsity

Next, we introduce an additional probability parameter C. Suppose each element Z is drawn as Z=0 with probability 1-C and X=1 with probability C.

Using this sparsity model, we define a modified matrix M'':

$$M'' = ZM' (2.25)$$

which means that only a fraction C of the entries in M' contribute to M''. The mean of each element in M'' remains zero, while its variance is computed as:

$$\operatorname{Var}(M_{i,j}'') = \operatorname{Var}(ZM_{i,j}') . \tag{2.26}$$

Since Z and $M'_{i,j}$ are independent, we can express the variance as:

$$Var(M''_{i,j}) = \mathbb{E}[X^2]\mathbb{E}[(M'_{i,j})^2] - \mathbb{E}[X]^2\mathbb{E}[M'_{i,j}]^2 . \tag{2.27}$$

Given that $\mathbb{E}[M'_{i,j}] = 0$, we simplify:

$$\mathbb{E}[X^2] = 1^2 C + 0^2 (1 - C) = C , \qquad (2.28)$$

which results in:

$$Var(M_{i,j}'') = C\sigma^2 . (2.29)$$

Thus, the normalized matrix takes the form:

$$\frac{M}{\sqrt{N}} = \frac{1}{\sigma\sqrt{NC}}M'' \,, \tag{2.30}$$

where again, the eigenvalues lie within a unit-radius circle centered at the origin. This derivation highlights how sparsity influences the spectral properties of the matrix.

Shifting the Eigenvalues and Stability Condition

Now, we define a new matrix:

$$B = M'' - dI (2.31)$$

where I is the identity matrix. This operation shifts the diagonal elements of M'' by -d, meaning they now have a mean of -d and variance $C\sigma^2$. The impact of this shift on the eigenvalues can be analyzed by considering:

$$\lambda_B = \lambda_{M''} - d \ . \tag{2.32}$$

When plotting the eigenvalues of B, we observe that a complete circular distribution only emerges when the variance of the diagonal elements approaches zero (see Figs. 2.3 and 2.4). This requirement ensures stability, which is formally expressed as:

$$\operatorname{Re}[\bar{\lambda}_{M''}] - d < 0 . \tag{2.33}$$

Since the largest eigenvalue of M'' lies at the boundary of a circle with zero mean and radius $\sigma\sqrt{NC}$, the stability condition simplifies to:

$$\sigma\sqrt{NC} < d. (2.34)$$

This inequality establishes the criterion for stability in terms of matrix parameters and the probability C, emphasizing how sparsity and shifting affect the system's stability. The condition ensures that no eigenvalue crosses the real-axis threshold at the origin, preventing instability.

To verify the stability condition Eq. (2.34), we performed numerical simulations using random interaction matrices. The elements of these matrices were drawn from both

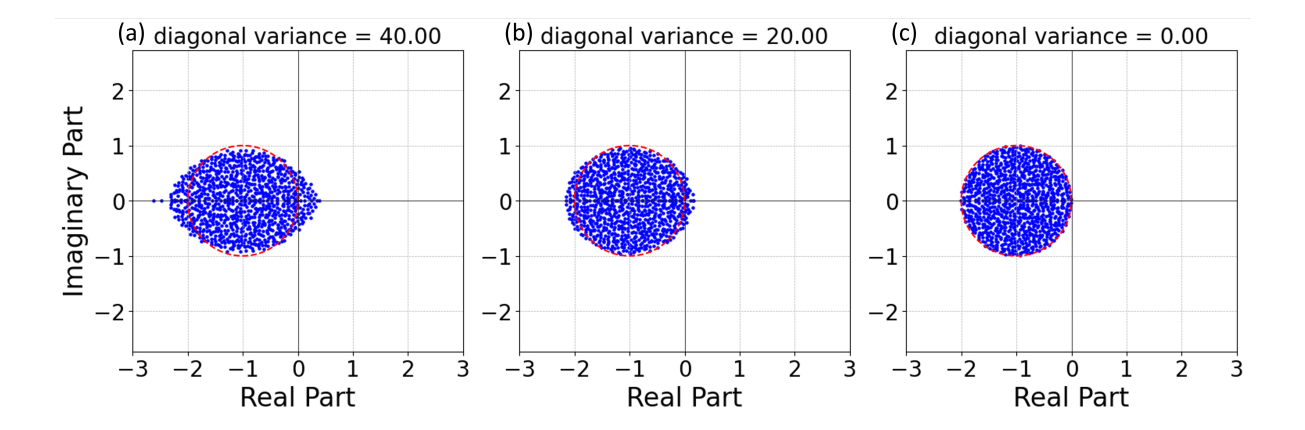


Figure 2.3: Eigenvalue distributions of sparse random matrices with normally distributed diagonal elements. The blue dots represent the rescaled eigenvalues, and the red dashed curves indicate the theoretical circular boundary with radius 1, centered at (-d,0) with d=1 in this case. Panels (a), (b), and (c) correspond to Diagonal variance = 0, 20, and 40. The matrix parameters are N=1000, connectivity C=0.2, and standard deviation $\sigma=1$.

normal and uniform distributions, and we analyzed the eigenvalue spectra to determine when instability occurs.

Figures 2.5 and 2.6 illustrate the comparison between the theoretical prediction and numerical results for normal and uniform distributions, respectively. Each figure consists of multiple panels representing different values of N. As the number of species increases, the results from numerical simulations converge towards the stability condition predicted by the theory. This agreement supports the asymptotic validity of the theoretical framework, consistent with the predictions of the Circular Law and the classical results of May [8] on the stability of large random ecosystems.

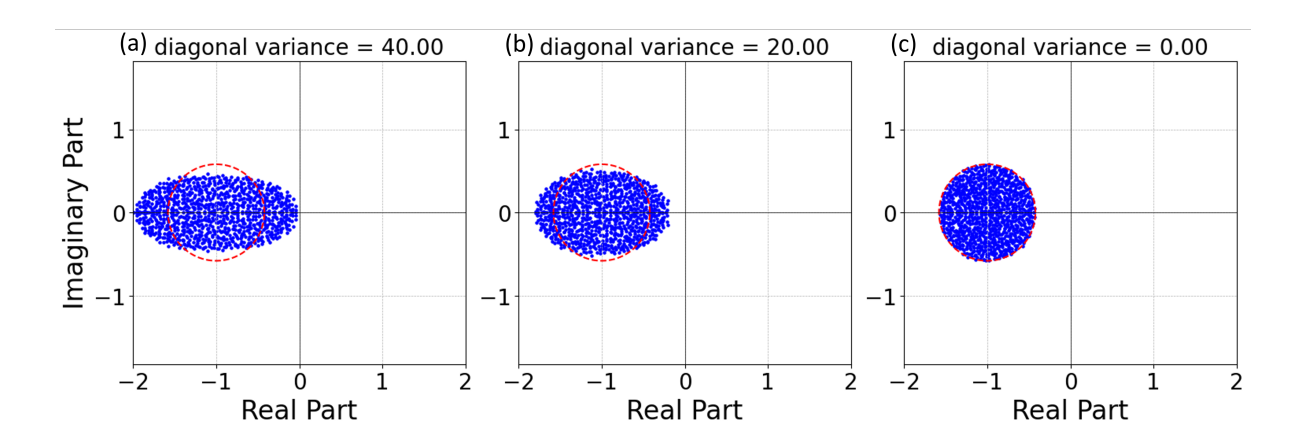


Figure 2.4: Eigenvalue distributions of sparse random matrices with uniformly distributed diagonal elements. The blue dots represent the rescaled eigenvalues, and the red dashed curves indicate the theoretical circular boundary with radius 0.58, centered at (-d,0) with d=1 in this case. Panels (a), (b), and (c) correspond to Diagonal variance = 0, 20, and 40. The matrix parameters are N=1000, connectivity C=0.2, and standard deviation $\sigma=1$. The elements are sampled from a uniform distribution in the range $[-\sigma,\sigma]$.

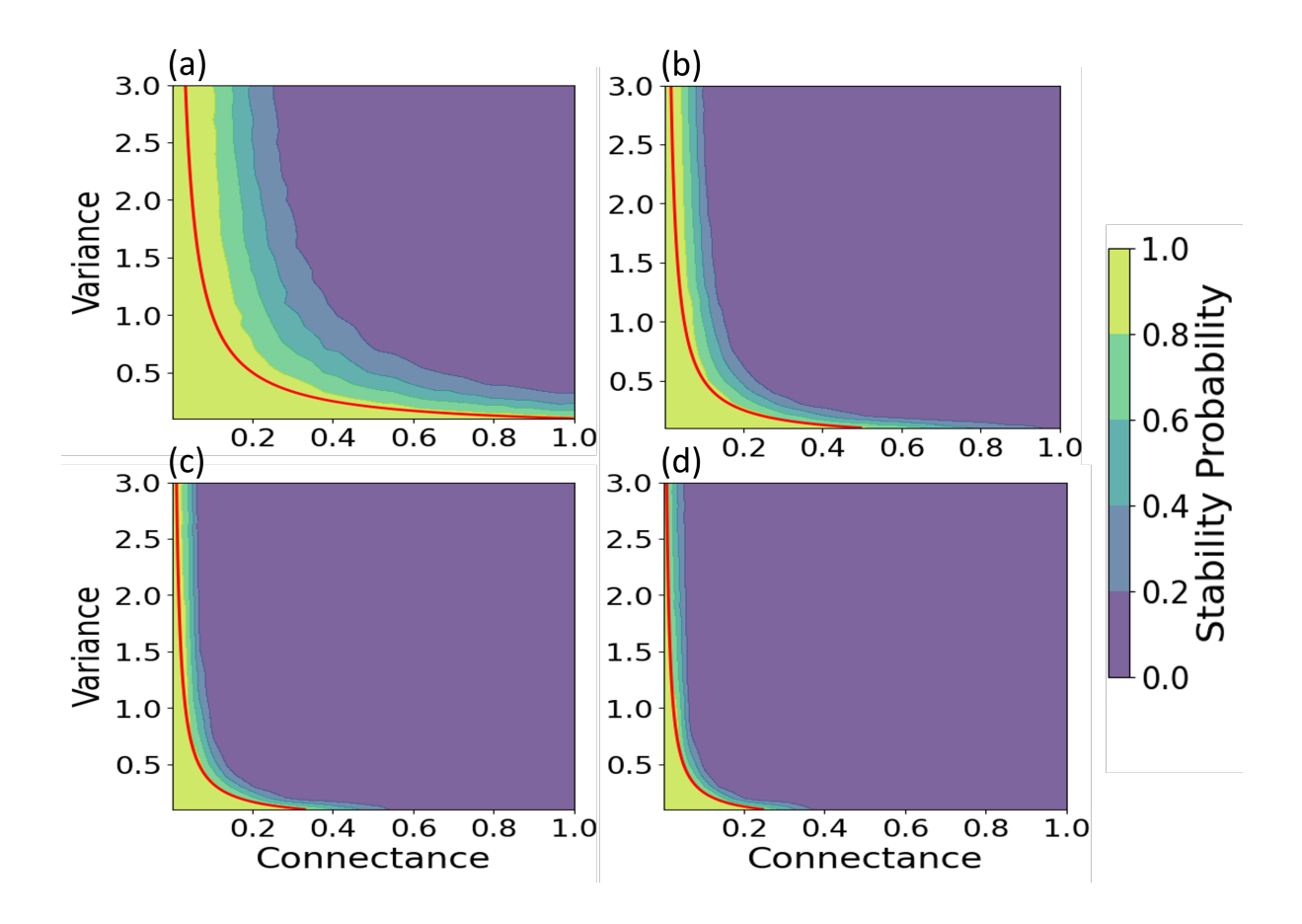


Figure 2.5: Stability probability as a function of connectance and variance for ecosystems with interactions sampled from a normal distribution with mean 0. Panels (a), (b), (c), and (d) correspond to ecosystems with 10, 20, 30, and 40 species, respectively. The red curve marks the analytical stability boundary based on theoretical predictions [Eq. (2.34)].

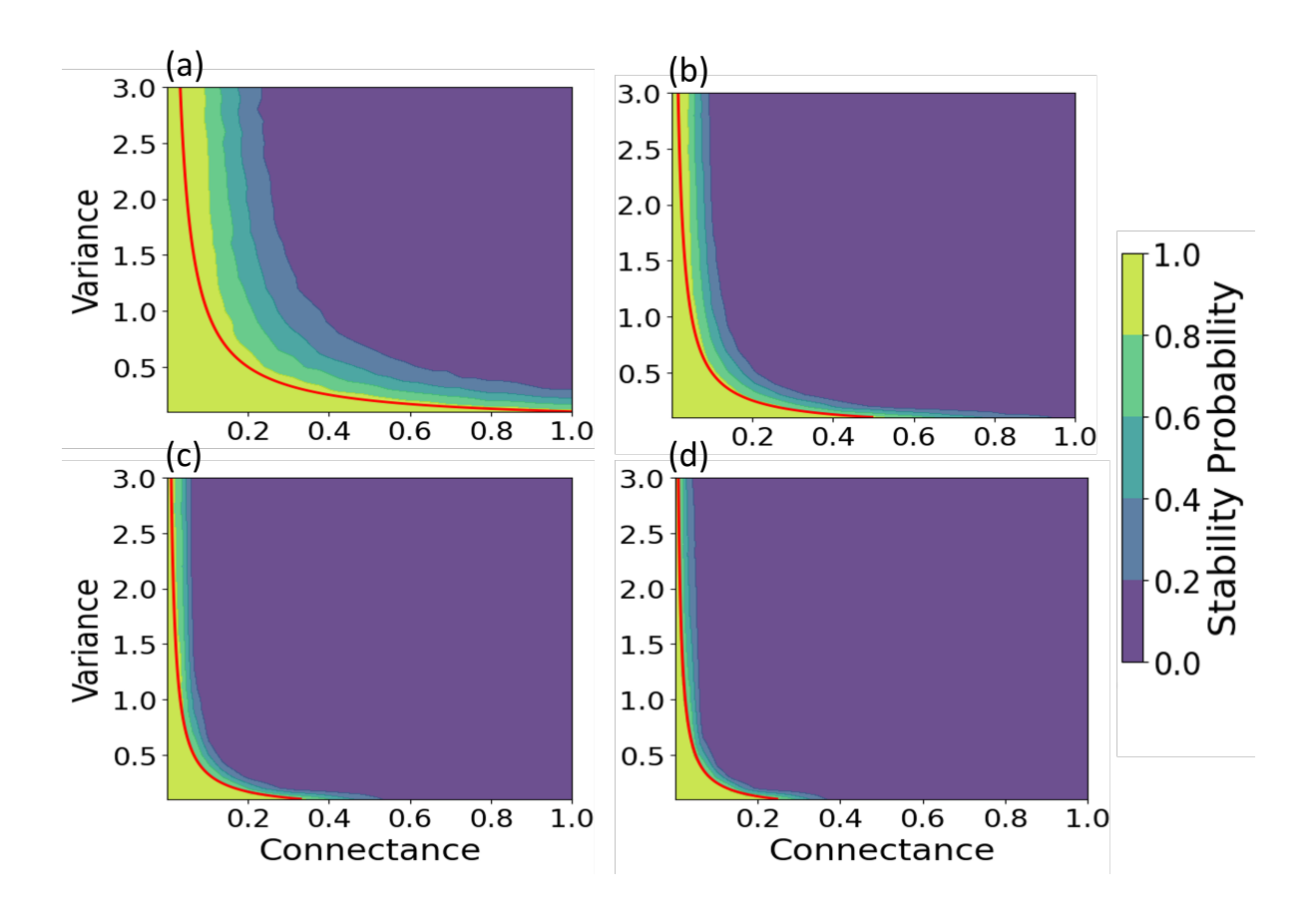


Figure 2.6: Stability probability as a function of connectance and variance for ecosystems with interactions sampled from a uniform distribution with mean 0. Panels (a), (b), (c), and (d) correspond to ecosystems with 10, 20, 30, and 40 species, respectively. The red curve marks the analytical stability boundary based on theoretical predictions [Eq. (2.34)].

2.11 Conclusion

In this chapter, we investigated the stability of large ecological systems using random matrix theory. We revisited May's framework and provided a detailed derivation of the stability condition, extending the analysis to include structural features such as sparsity, variance scaling, and diagonal shifts. We complemented this theoretical work with numerical simulations, which validated the predictions and demonstrated how these structural parameters influence the eigenvalue spectrum and, consequently, the stability of complex ecosystems.

While this spectral approach offers powerful insights into system-level patterns, it abstracts away species-specific interactions and ecological mechanisms. In the next chapter, we turn to consumer-resource models to explore the dynamics of species competition and the conditions under which coexistence or exclusion occurs in ecosystems with shared limiting resources.

Chapter 3

Competitive exclusion principle

3.1 Introduction

Having examined global stability through statistical models in the previous chapter, we now shift to a mechanistic understanding of species interactions at the steady state. This chapter focuses on the classical Competitive Exclusion Principle (CEP), which states that two species competing for the same limiting resource cannot coexist indefinitely under constant environmental conditions [15, 16].

The goal of this chapter is to analytically characterize the conditions under which species coexist or exclude one another in simple consumer-resource systems, and to interpret these results geometrically and biologically. By steady state, we mean a condition where species abundances and resource levels remain constant over time, assuming no further perturbations.

We study coexistence and exclusion using the consumer-resource model [17, 18], which

allows us to track species abundances and resource levels over time until they reach a steady state. We analyze systems with one or two species competing for one or two resources, and derive analytical conditions for the stationary states of these systems. Using geometric tools such as Zero Net Growth Isoclines (ZNGIs) [18], we interpret how resource supply, species traits, and consumption dynamics determine whether species coexist or whether one excludes the other.

To illustrate this idea, consider the following scenario:

In a remote village, two families share a single well. One family wakes early, uses water efficiently, and wastes none. The other needs more, arrives late, and loses water to evaporation. As the dry season continues, the well runs low. Eventually, only one family remains — not because the other didn't try, but because they couldn't survive on what was left.

This is the essence of the Competitive Exclusion Principle: when two groups compete for the same limited resource, the one that survives with less will outlast the other.

This approach provides a concrete and biologically grounded framework for understanding coexistence in ecological communities, and sets the stage for exploring how additional factors like spatial structure and migration might alter these outcomes.

3.2 Consumer-Resource Model

In this section, we write the dynamical equations of n number of species competing for r number of resources (i.e., the consumer-resource model):

$$\frac{1}{N_i} \frac{dN_i}{dt} = r_i \sum_{j=1}^r \frac{R_j}{R_j + k_i} - m_i , \qquad (3.1)$$

$$\frac{dR_j}{dt} = a(S_j - R_j) - \sum_{i=1}^n \frac{r_i N_i}{\gamma_i} \frac{R_j}{R_j + k_i} , \qquad (3.2)$$

where N_i is the population density of species i, R_j is the availability (in concentration) of resource j, r_i is the growth rate of species i, m_i is the mortality-rate of species i, γ_i is the number of individuals of species i produced per unit of resource consumption, S_j is the amount of resource j being supplied to the system, a is the rate constant for resource supply, and k_i is the resource availability at which growth-rate of species i reaches half of its value; therefore, we call k_i as the the half saturation constant. On the right-hand side (RHS) of Eq. (3.1), the first and second terms, respectively, represent the growth-and mortality-rate of species i. The first and second terms on the RHS of Eq. (3.2) represent the supply and consumption rate of resource j respectively.

To predict the stationary-state outcome of resource competition via Eqs. (3.1) and (3.2), we need four pieces of information. These are the reproductive or growth response of each species to the resources the first term on RHS of Eq. (3.1), the mortality rate of each species, the supply rate S_j of each resource, and the consumption rate r_i of each resource by each species. Then, the stationary-state is reached when the resource-dependent reproduction of each species balances its mortality-rate. Additionally, when resource supply balances the total resource consumption for each resource. Mathematically, these stationary-state conditions can be written using Eqs. (3.1) and (3.2) as

follows:

$$r_i \sum_{j=1}^r \frac{R_j^*}{R_j^* + k_i} = m_i , \qquad (3.3)$$

$$a(S_j - R_j^*) = \sum_{i=1}^n \frac{r_i N_i^*}{\gamma_i} \frac{R_j^*}{R_j^* + k_i} , \qquad (3.4)$$

where N_i^* and R_j^* are the stationary-state population density of species i and availability of resource j respectively.

Notice that the stationary-state $\{N_i^*, R_j^*\}_{i,j}$ can be either stable or unstable. This depends on the fact that if we perturb our system from its stationary-state, then, if the system goes away from its stationary-state, this stationary state will be unstable; otherwise, it is stable [36].

3.3 Competition for a single resource

In the previous section, we introduced the general dynamical equations for n species competing for r resources in the consumer-resource model [Eqs. (3.1) and (3.2)]. While this model provides a comprehensive framework for understanding multispecies competition, analyzing the system may become complex due to the interactions between multiple species and resources.

To gain deeper insight of the system, it is useful to first explore a simpler case. To this end, we first focus on the interaction between a single species and a single resource. This reduced model captures the essential dynamics of resource competition while allowing us to derive analytical expressions for the stationary-state conditions. By examining

this simpler scenario, we can develop intuition that will later guide our understanding of more complex multispecies interactions.

3.3.1 One species and one resource

To analyze the steady-state behavior of a single species competing for a single resource, we focus directly on the stationary-state condition for the population N and the resource concentration R. At stationary state, the system reaches a condition where the species' growth rate is balanced by its mortality rate, and the resource supply is balanced by the consumption rate. These stationary-state conditions are represented by the following equations:

$$rN\frac{R^*}{R^*+k} - mN^* = 0 , (3.5)$$

$$a(S - R^*) - \frac{rN^*}{\gamma} \frac{R^*}{R^* + k} = 0.$$
 (3.6)

Here, we have two equations and two unknowns: R^* and N^* . When we solve both equations, we get the equilibrium values of R^* and N^* as:

$$R^* = \frac{mk}{r - m} \,, \tag{3.7}$$

$$N^* = \frac{a\gamma(S - R^*)}{r} \frac{R^* + k}{R^*} , \qquad (3.8)$$

For a real system, it is essential that both R^* and N^* should be positive. Thus, from Eqs. (3.7) and (3.8), we can derive the necessary conditions for the positivity of R^* and N^* : r must be greater than m and the resource supply S must exceed R^* [Eq. (3.8)].

Figure 3.1a demonstrates a scenario where the resource supply is insufficient to sustain

the population [i.e., $S < R^*$, see Eq. (3.8)]. As a result, the population density declines towards zero indicating extinction while the resource concentration stabilizes to a non-zero value [(3.7)].

Figure 3.1b illustrates a contrasting scenario where the resource supply is sufficient. Here, the system reaches a stable stationary state where both the population and resource stabilize at non-zero values as predicted by Eqs. (3.8) and (3.7).

The above two discussed scenarios highlight how the availability of resources determines the fate of the species. In Fig. 3.1a, the limited resource supply leads to species extinction, while in Fig. 3.1b, sufficient resource supply results in a stable population and resource concentration. These results align with the analytical expressions for the stationary-state values of N^* and R^* derived earlier [Eqs. (3.7) and (3.8)], demonstrating how resource availability plays a critical role in the long-term dynamics of the population and resource in the system.

3.3.2 Two species and one resource

Building upon the insights from the previous subsection, which examined the dynamics of a single species competing for a single resource, we now extend our analysis to two species competing for the same resource. The foundational understanding of how resource availability impacts population dynamics become essential in this context. In the one-species model, we established the critical conditions for species survival based on resource supply and growth rate. As we transition to the two-species model, these principles will illuminate the competitive interaction between species and the influence of resource distribution on their coexistence or exclusion.

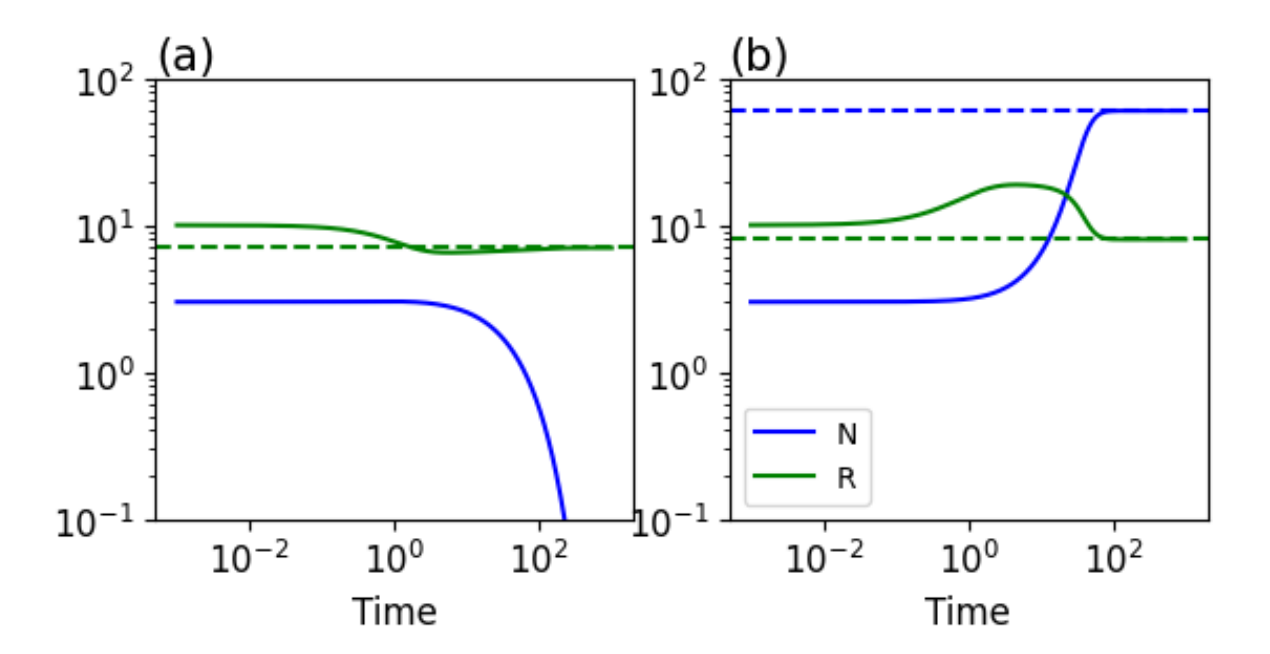


Figure 3.1: Time evolution of population density (blue) and resource concentration (green) for a one-species one-resource model. (a) When the resource supply is insufficient $(S = 7 < R^*)$, the population density declines to extinction $(N \to 0)$, while the resource concentration stabilizes at a non-zero value, as predicted by Eq. (3.7). (b) When the resource supply is sufficient $(S = 20 > R^*)$, both the population and resource concentrations stabilize at non-zero values, as predicted by Eqs. (3.8) and (3.7). Solid lines represent the population and resource dynamics over time, while dashed lines represent the stationary-state values derived from the analytical solutions [Eqs. (3.7) and (3.8)]. The parameters used are growth rate r = 0.4, mortality rate m = 0.2, half-saturation constant k = 8, resource supply rate constant a = 1, and resource consumption efficiency $\gamma = 1$. The dynamics [Eqs. (3.1) and (3.2)] were solved via numerical integration using Euler's method (see Appendix 6).

To analyze the competition between two species for a single resource, we start with the stationary state conditions derived from Eqs. (3.1) and (3.2). These conditions are expressed as follows:

$$r_i N_i^* \frac{R^*}{R^* + k_i} - m_i N_i^* = 0 , (3.9)$$

$$a(S - R^*) - \sum_{i=1}^{2} \frac{r_i N_i^*}{\gamma_i} \frac{R^*}{R^* + k_i} = 0.$$
 (3.10)

From the Eq. (3.9), we derive the stationary state resource concentration R^* :

$$R^* = \frac{m_i k_i}{r_i - m_i} \ . \tag{3.11}$$

This indicates how the resource concentration depends on species-specific parameters: the growth rate r_i , the mortality rate m_i , and the half-saturation constant k_i .

When both species have different value of R^*

Here, we focus on a case of two species (with different R^*) competing for one resource. In Eq. (3.10), we need to determine two unknowns $N_{1,2}^*$ after substituting the value of R^* from Eq. (3.11). At this point, we have one equation and two unknowns. To solve this equation, we need to set one of the unknowns equal to zero. We decide which N_i to set to zero based on the value of R^* : the species with the greater value of R^* will have its population density set to zero, as observed in our simulations (see Fig. 3.2). In this case, the population density of the other species is given by:

$$N^* = \frac{a\gamma(S - R^*)}{r} \frac{R^* + k}{R^*} \ . \tag{3.12}$$

Here k is the half-saturation constant corresponding to the survived species. We get above equation from Eq. (3.10). When we have two different species competing for a single resource, and both species have different value of R^* , only one species will survive. In this scenario, the species with the lower value of R^* will outcompete the other species, displacing it from the habitat. This phenomenon, known as competitive exclusion, means the fittest species—defined by having the lower R^* —outcompetes the other.

Figure 3.2 clearly shows this process. At first, when the resource levels are above R_2^* , both species grow, as seen in the blue and orange lines. However, as they consume resources, the levels start to drop. Species 1's reaches its maximum when resources reach R_1^* , while species 2 can keep growing until the resources hit R_2^* . When that happens, species 1 can't find enough resources to survive and is displaced by species 2. This example illustrates how having different resource thresholds can lead to one species outcompeting the other.

When both species have the same value of R^*

When both species have the same value of R^* [Eq. (3.11)], the population densities of both species will be non-zero because the resource availability is sufficient to support both species. This occurs under the assumption that the resource is abundant enough, allowing for coexistence rather than competitive exclusion. In this case, we obtain a constraint for both species when solving Eq. (3.10):

$$\frac{r_1 N_1^*}{\gamma_1} \frac{R^*}{R^* + k_1} + \frac{r_2 N_2^*}{\gamma_2} \frac{R^*}{R^* + k_2} = a(S - R^*) . \tag{3.13}$$

If the value of R_1^* and R_2^* are same, then the initial resource level is greater than R_1^* (or R_2^*), both species will increase in population density. As the population size increase,

the resource level decreases. The population size of species 1 and species 2 will stop increasing when the resource level decreases to R_1^* (or R_2^*). In this case, both species can coexist because the resource level does not fall below R_1^* (or R_2^*). Both species will have sufficient resources to maintain stable populations.

Figure 3.2(b) shows this situation, where both species grow together as there are plenty of resources. The blue and orange lines rise until the resource levels drop to R_1^* (or R_2^*). At this point, both species reach a stable population size, as shown by the flattening of the curves. The resource level stays above R^* , allowing both species to thrive together, highlighting how sharing resources can help maintain diversity among species.

3.4 Competition for two resources

In this section, we explore how n species compete for two resources in a habitat. If the available resources in the habitat are less than what is required for a species to survive, the species will die. Therefore, the correct balance of resources is essential for the existence of species in a particular habitat. This balance is described by the Zero Net Growth Isocline (ZNGI), which represents the conditions where a species's growth rate equals its mortality rate. A species can survive only if the resource supply point is above the ZNGI; otherwise, it will not be able to maintain a stable population and will eventually die. We will examine this condition in two scenarios: first, when only one species present in the habitat, and second, when two species present in the habitat.

If we extend Eq. (3.1) and Eq. (3.2) to model the consumption of two resources by n

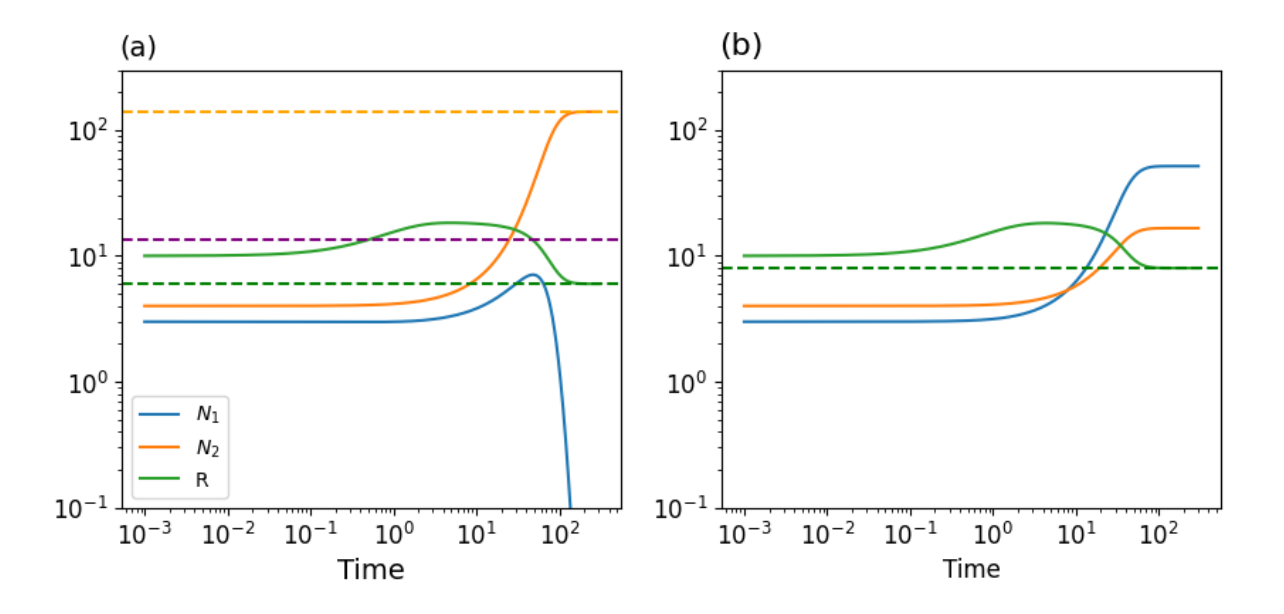


Figure 3.2: Dynamics of two competing species and a single shared resource. Species 1: Blue. Species 2: Orange. Resource: Green. Panel (a) illustrates a situation where species 1 has a higher resource concentration threshold/requirement $(R_1^* > R_2^*)$, derived from Eq. (3.11). Here, the purple dashed line represents R_1^* , while the green dashed line is for R_2^* . Panel (b) depicts a scenario where both species have the same resource concentration threshold $(R_1^* = R_2^*)$. Dashed lines in panel (a) represent the stationary-state values for population densities and resource levels derived from the analytical solutions [Eqs. (3.12) and (3.11)] and in panel (b) there is only one dashed line which represents resource level derived from the analytical solution [Eqs. (3.11)]. The parameters used are growth rates $r_1 = 0.4$ and $r_2 = 0.2$, mortality rates $m_1 = 0.25$ and $m_2 = 0.1$, half-saturation constants $k_1 = 8$ and $k_2 = 6$, resource consumption efficiencies $\gamma_1 = \gamma_2 = 1$, resource supply rate constant a = 1 and resource supply S = 20. For panel (b) all other parameters are same except $m_1 = 0.2$ and $k_2 = 8$. The dynamics [Eqs. (3.1) and (3.2)] were solved via numerical integration using Euler's method (see Appendix 6).

species, the resulting equations are:

$$\frac{1}{N_i} \frac{dN_i}{dt} = r_i \sum_{j=1}^{2} \frac{R_j}{R_j + k_i} - m_i , \qquad (3.14)$$

$$\frac{dR_j}{dt} = a(S_j - R_j) - \sum_{i=1}^n \frac{r_i N_i}{\gamma_i} \frac{R_j}{R_j + k_i} . {(3.15)}$$

We will now solve these equations for two cases: n = 1 or one species (see Sec. 3.4.1) and n = 2 or two species (see Sec. 3.4.2).

3.4.1 Two resources and one species

Before we consider competition between multiple species, it is helpful to understand how a single species interacts with two resources in the environment. This will provide the foundation for analyzing more complex scenarios where multiple species compete for the same resources.

To analyze the stationary-state behavior of a single species interacting with two resources, we focus directly on the stationary-state condition for the population N and the resource concentrations R_1 and R_2 . At this stationary state, the growth rate of the species is balanced by its mortality rate, and the resource supply is balanced by the consumption rate. These stationary-state conditions are represented by the following

equations:

$$r\sum_{j=1}^{2} \frac{R_{j}^{*}}{R_{j}^{*} + k} - m = 0 , \qquad (3.16)$$

$$a(S_j - R_j^*) - rN^* \frac{R_j^*}{R_j^* + k} = 0. (3.17)$$

From Eq. (3.16), we derive the zero net growth isocline (ZNGI). Figure 3.3 displays the zero net growth isocline (ZNGI), derived from Eq. (3.16), indicating the boundary between population stability and decline.

Equation (3.17) shows the stationary state population of species N^* as a function of R_1^* and R_2^* . Additionally, we impose the condition that at stationary state, the population density of the species must be greater than zero; otherwise, the species cannot persist over time:

$$N^* = \frac{a(S_j - R_j^*)(R_j^* + k)}{rR_j^*} > 0.$$
 (3.18)

In Eq. (3.18), we see that N^* remains positive when $S_j > R_j^*$ for j = 1, 2. Therefore, when the supply point lies below or on the ZNGI (see Fig. 3.3), the species cannot sustain a positive population density. This emphasizes the critical resource levels required for the species' survival, highlighting the importance of resource availability in maintaining stable population dynamics.

Figure 3.4 demonstrates how the population density of a single species and the resource levels evolve at different supply points (A, B, and C from Fig. 3.3).

In Fig. 3.4a, we observe that the population density of the species approaches zero over time. This decline indicates that the corresponding supply point is below the zero

net growth isocline (see Fig. 3.3). Consequently, the species cannot sustain a positive population density under these conditions. Similarly, Fig. 3.4b also shows a decrease in population density, suggesting that this supply point fails to support the species.

In contrast, Fig. 3.4c illustrates a scenario where the population density stabilizes over time, indicating that the conditions at this supply point are sufficient for the species to persist. This behavior aligns with the stationary-state conditions described in Eq. (3.17).

Overall, Fig. 3.3 underscores the critical relationship between resource availability and population stability, emphasizing that supply points below or on the ZNGI lead to population decline, while points above this threshold can support a stable population.

3.4.2 Two resources and two species

Having examined the dynamics of one species competing for two resources, we now extend this understanding to a scenario where two species compete for two resources. This allows us to explore the potential for coexistence or competitive exclusion between species in a shared environment.

To analyze the stationary-state behavior of two species interacting with two shared resources, we consider the stationary-state conditions for the populations N_1 , N_2 , and resource concentrations R_1 , R_2 . At stationary state, the growth rate of each species balances with its mortality rate, and the resource supply balances with consumption. These stationary-state conditions are represented by the following equations:

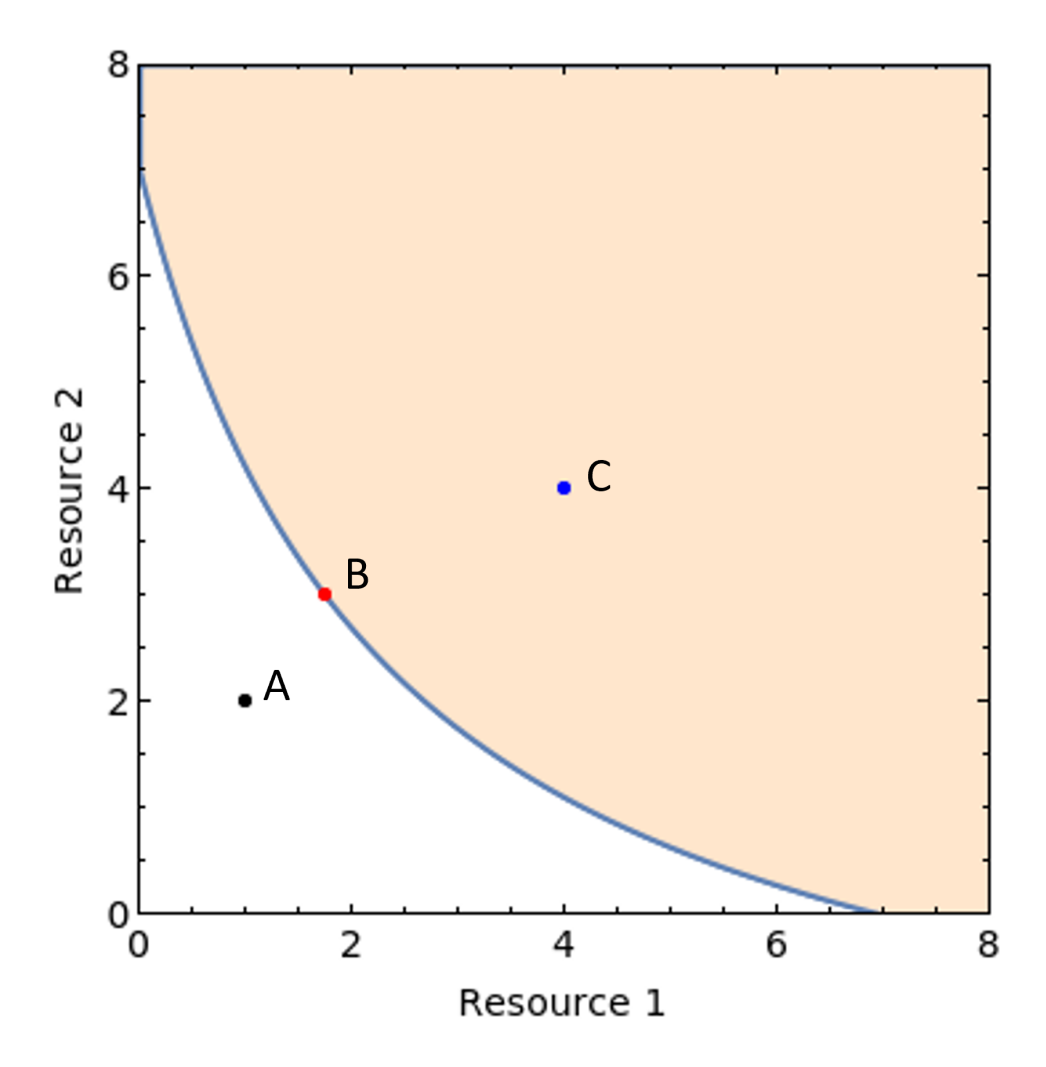


Figure 3.3: The zero net growth isocline (ZNGI), derived from Eq. (3.16), indicating the conditions under which the species can maintain a stable population of one species. Points A, B, and C represent distinct supply points. The parameters used are growth rate r = 0.4, mortality rate m = 0.2, resource saturation constant k = 7.0, and resource supply a = 1.

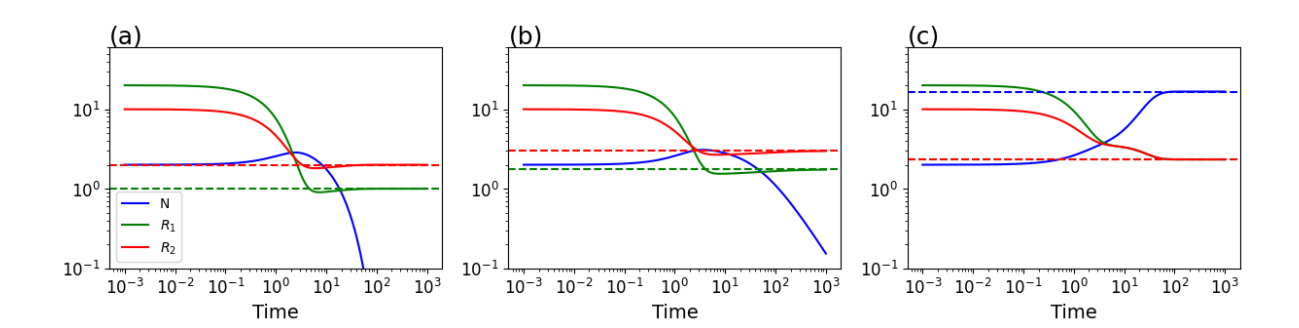


Figure 3.4: Population density and resource levels at supply points A, B, and C (see Fig. 3.3) as functions of time. Panels (a), (b), and (c) illustrate the system's behavior at these respective supply points. Dashed lines represent the analytical values [obtained numerically by solving Eq. (3.16)] of resources and the species' population density at the stationary state, as described by Eq. (3.18). The parameters used in this figure are the same as those specified in Fig. 3.3. The dynamics [Eqs. (3.1) and (3.2)] were solved via numerical integration using Euler's method (see Appendix 6).

$$r_i \sum_{j=1}^{2} \frac{R_j^*}{R_j^* + k_i} - m_i = 0, \quad (i = 1, 2),$$
 (3.19)

$$a(S_j - R_j^*) - \sum_{i=1}^2 r_i N_i^* \frac{R_j^*}{R_j^* + k_i} = 0, \quad (j = 1, 2).$$
 (3.20)

From Eq. (3.19), we derive the zero net growth isocline (ZNGI) for both species. We can then express N_1^* and N_2^* as functions of the resource concentrations R_1^* and R_2^* by

Eq. (3.20) The stationary-state populations are given by:

$$N_1^* = \frac{a(S_1 - R_1^*) \frac{R_2^*}{R_2^* + k_2} - a(S_2 - R_2^*) \frac{R_1^*}{R_1^* + k_2}}{r_1 \left[\frac{R_1^*}{R_1^* + k_1} \frac{R_2^*}{R_2^* + k_2} - \frac{R_1^*}{R_1^* + k_2} \frac{R_2^*}{R_2^* + k_1} \right]} > 0 ,$$
(3.21)

$$N_2^* = -\frac{a(S_1 - R_1^*) \frac{R_2^*}{R_2^* + k_1} - a(S_2 - R_2^*) \frac{R_1^*}{R_1^* + k_1}}{r_2 \left[\frac{R_1^*}{R_1^* + k_1} \frac{R_2^*}{R_2^* + k_2} - \frac{R_1^*}{R_1^* + k_2} \frac{R_2^*}{R_2^* + k_1} \right]} > 0.$$
(3.22)

These expressions, Eqs. (3.21) and (3.22), show how population densities depend on resource availability and species' parameters, determining whether species coexist or one competitively excludes the other.

Figure 3.5 establishes the framework by illustrating the zero net growth isoclines (ZNGI) for both species. The intersections of these isoclines, marked as Points A and B, are pivotal as they represent the stationary states where each species can sustain itself based on the available resources.

Figure 3.6 delves into the stability of these stationary points (in Fig. 3.5) under different supply levels. It indicates that stability is highly contingent on the combination of resource supply rates S_1 and S_2 . The observed outcomes demonstrate that certain supply combinations can either stabilize the populations or lead to declines, emphasizing the critical nature of resource availability in determining competitive interactions.

In Fig. 3.7, ZNGI is explored across multiple supply points, illustrating the feasible solutions derived from the stationary-state conditions. The shaded regions highlight the circumstances under which both species can coexist, while the lines indicate ZNGI. When the stationary solution (marked by circles) lies in that feasible region, both species survive.

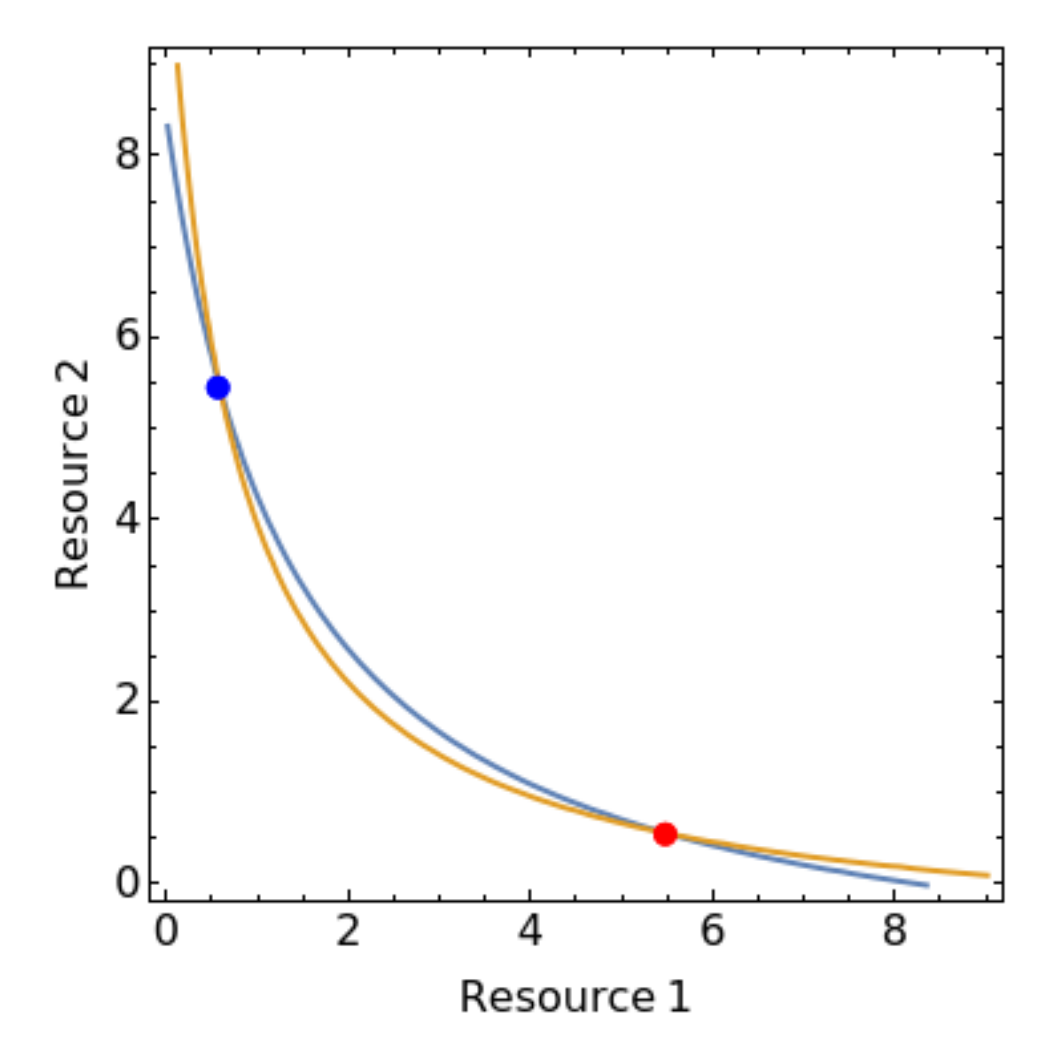


Figure 3.5: Contour plot for the competition for two resources between two species. The blue and orange curves represent the Zero Net Growth Isoclines (ZNGIs) [Eq. (3.19)] for each species. The blue and red points indicate the intersection of the ZNGIs, highlighting potential stationary states of resource availability for the two species. The parameters used are growth rates $r_1 = 0.4$ and $r_2 = 0.2$, mortality rates $m_1 = 0.25$ and $m_2 = 0.15$, resource carrying capacities $k_1 = 5$ and $k_2 = 3.5$, and resource supply rate constant a = 1.

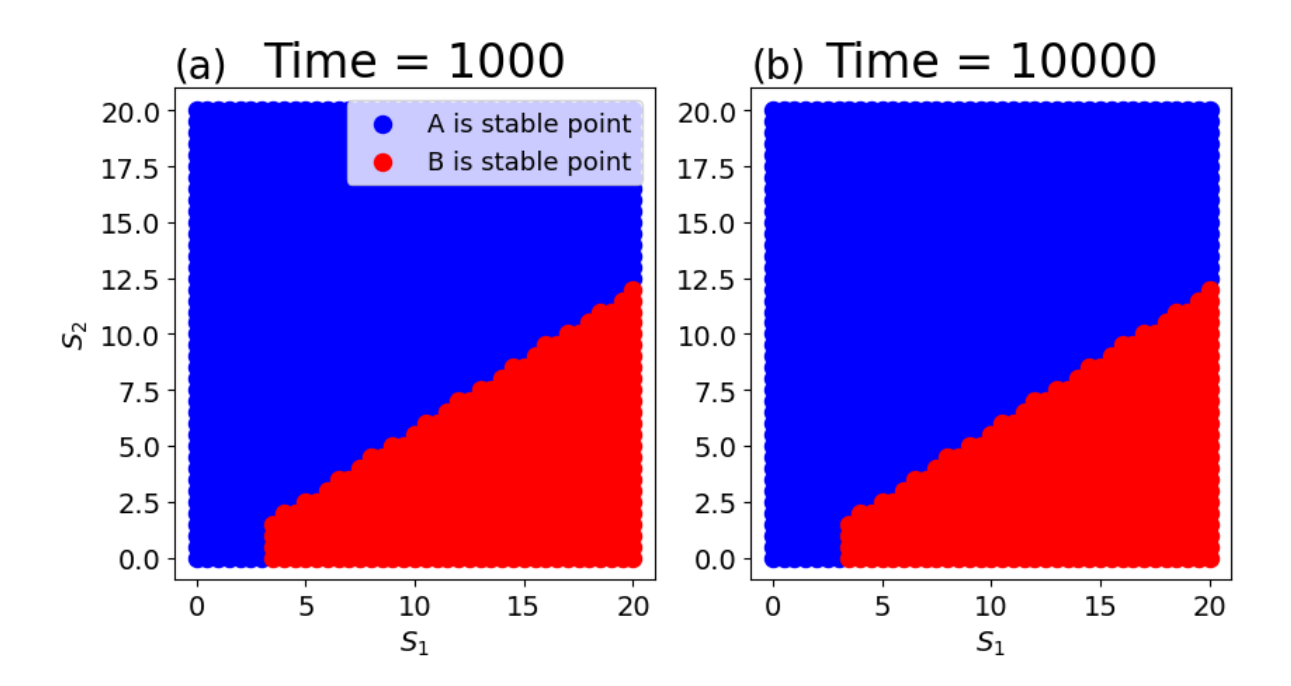


Figure 3.6: Stability of stationary Points A and B (Point A and B are the same points as shown in Fig. 3.5) under different supply levels S_1 and S_2 , represented in panels (a) and (b). Each panel examines different combinations of supply levels across two time intervals: 1000 and 10,000 time units. The parameters used in this figure are the same as those specified in Fig. 3.5.

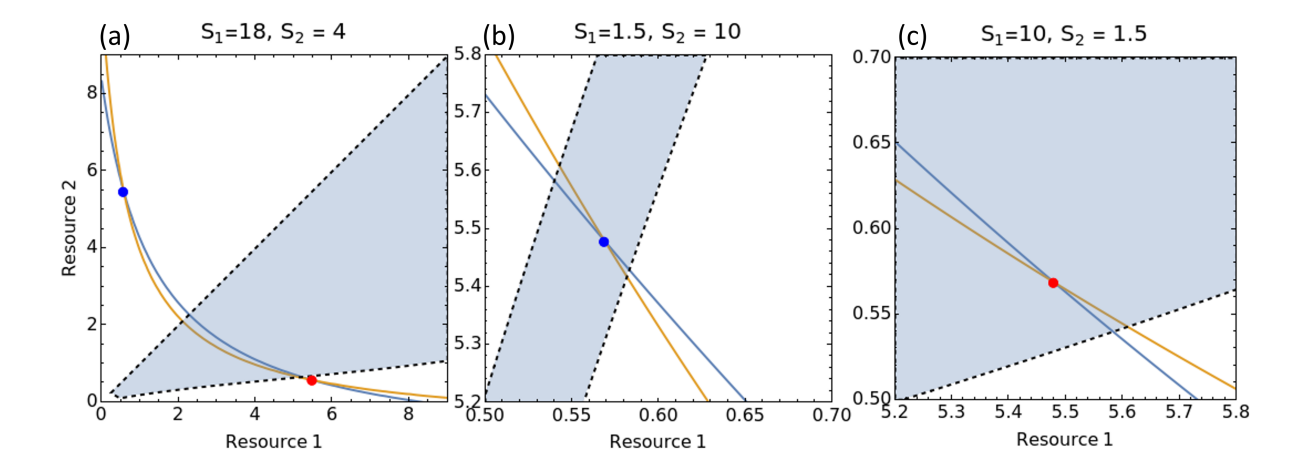


Figure 3.7: The zero net growth isoclines (ZNGIs) (Fig. 3.5) for both species for different supply points, as shown in panels (a), (b), and (c). The orange and blue lines represent the ZNGI for species 1 and species 2, respectively [Eq. (3.19)]. The shaded regions indicate the feasible solutions obtained from Eqs. (3.21) and (3.22). The parameters used in this figure are the same as those specified in Fig. 3.5.

Figure 3.8 displays the species populations under various resource supply scenarios. It reveals that under specific conditions, both species can thrive, as demonstrated by Points A and B being situated within the feasible region (as discussed in Fig. 3.7). Conversely, scenarios where one species declines illustrate the potential for competitive exclusion, underscoring how sensitive these dynamics are to resource supply levels.

Finally, we extend our analysis (shown in Fig. 3.8) for different supply points (S_1, S_2) . Figure. 3.9 portrays the temporal evolution of the system, showcasing the gradual shift from coexistence to competitive exclusion over time. As time progresses, the coexistence region shrinks, indicating that competitive pressures can escalate, resulting in the decline of one or both species in areas where resources are limited.

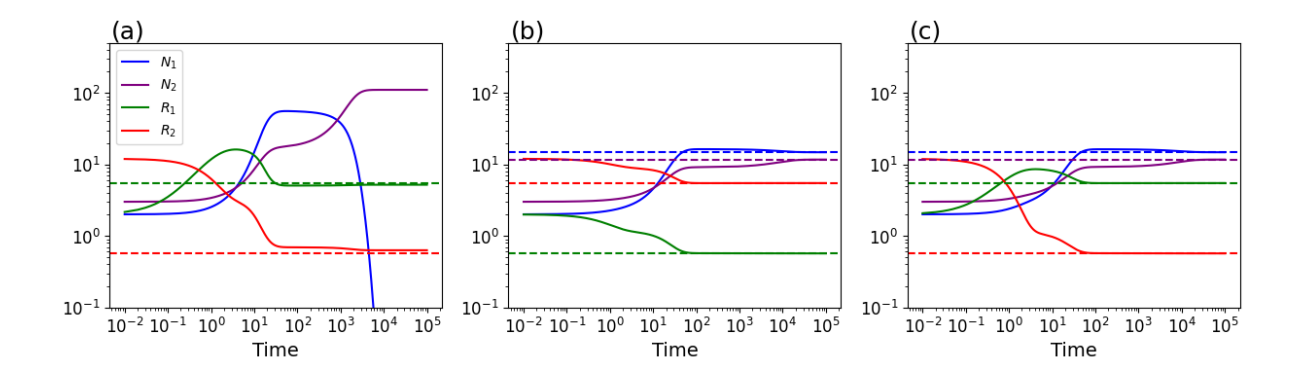


Figure 3.8: The dynamics of the two resources and two species model under various supply conditions. In panel (a), the population of species 1 declines, indicating that both stable points lies outside the feasible region Fig. 3.7(a). In panel (b), both species survive as the population is supported by Point A, which is located within the feasible region Fig. 3.7(b). Panel (c) also shows both species surviving, this time due to Point B being situated in the feasible area Fig. 3.7(c). The parameters used in this figure are the same as those specified in Fig. 3.5. The dynamics [Eqs. (3.1) and (3.2)] were solved via numerical integration using Euler's method (see Appendix 6).

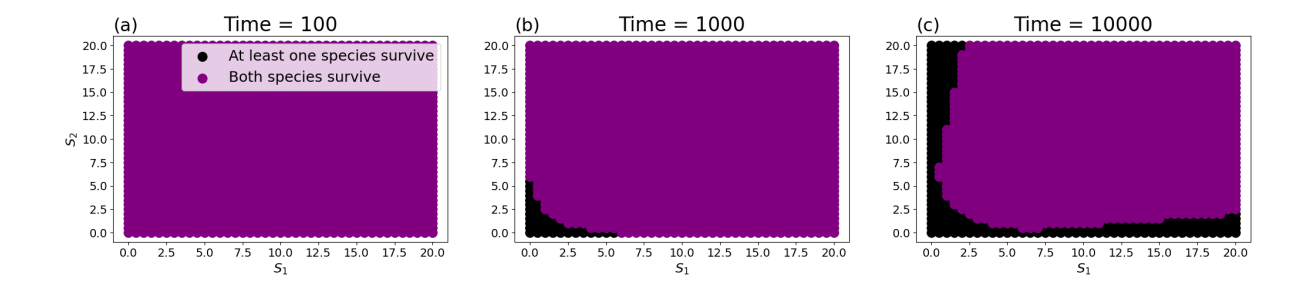


Figure 3.9: Number of surviving species (out of two) competing for two shared resources at three different times: (a) Time = 100, (b) Time = 1000, and (c) Time = 10000. The region colored in purple represents areas where both species survive, while the black regions indicate areas where at least one species survives. The parameters used in this figure are the same as those specified in Fig. 3.5. We keep the species population's threshold 10^{-10} , such that if the population is below this threshold, we consider that species is extinct.

3.5 Conclusion

This chapter provided a detailed analysis of the competitive exclusion principle using consumer-resource dynamics. We demonstrated how coexistence depends on species-specific parameters such as growth rates, mortality, half-saturation constants, and resource availability. The Zero Net Growth Isocline (ZNGI) approach offered a visual and analytical framework for interpreting stationary states and extinction thresholds.

However, these models assume spatially isolated communities. In reality, migration between habitats is common and can change competition outcomes. In the next chapter, we incorporate spatial structure via patch-based models and explore how asymmetric migration facilitates coexistence, even in systems where classical models predict exclusion.

Chapter 4

Species Coexistence via Asymmetric Migration

4.1 Introduction

The previous chapter showed how resource competition determines whether species coexist or exclude one another. However, real ecosystems are spatially structured, and individuals often migrate between habitats. Migration can modify local interactions and enable coexistence under otherwise exclusionary conditions [37, 38].

In this chapter, we explore species coexistence through asymmetric migration between two patches. By asymmetric migration, we mean that the rate at which individuals move from patch A to patch B is not necessarily equal to the rate from B to A. Using a two-patch Lotka–Volterra competition model, we study how different migration rates affect the stationary states — the long-term equilibrium of species densities in each patch —

and the stability of the system. We derive analytical coexistence conditions and interpret how migration reshapes effective competition. This analysis highlights spatial movement as a novel mechanism for promoting biodiversity.

To motivate this idea, consider a continuation of the earlier village story:

After one family is forced to leave the original well, they travel to a neighboring village where another well exists. This new well is smaller and harder to reach, but it provides just enough water to sustain them. Over time, the two families begin to move between the two wells depending on the season and need.

Now, instead of one family being excluded, both survive — not by sharing a single limited resource, but by spreading out and using resources in space. This is how migration can support coexistence even when competition alone would lead to exclusion.

Through this lens, we show that spatial movement allows species to reduce direct competition and create conditions for coexistence that would not emerge in a single, well-mixed environment.

4.2 Asymmetric Migration Model

In this section, we explore how migration plays an important role in the coexistence of species. To this end, we consider a habitat, where two species are competing for a single resource. Additionally, to introduce the concept of spatial migration, we divide this

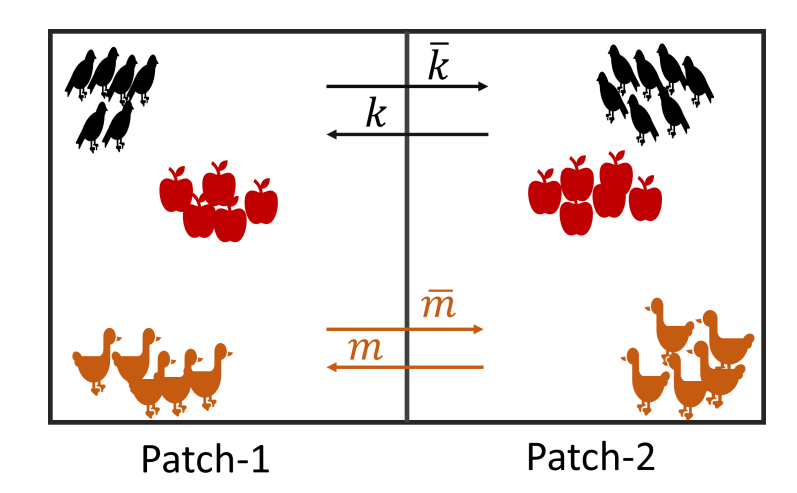


Figure 4.1: Illustration of asymmetric migration dynamics between two patches. The schematic shows two patches, patch-1 and patch-2, each containing two species (birds and ducks) and a shared resource (apples). Arrows represent migration between patches, with black arrows for the bird migration and brown arrows for the duck migration. The direction of the arrows indicates the direction of migration, while the parameters k, \bar{k} , m, and \bar{m} represent the migration rates. Specifically, \bar{k} and k denote the migration rates of species 1 (birds) from patch-1 to patch-2 and from patch-2 to patch-1, respectively, while \bar{m} and m denote the migration rates of species 2 (ducks) from patch-1 to patch-2 and from Patch-2 to Patch-1, respectively.

habitat into two parts, referred to as *patch-1* and *patch-2* (see Fig. 4.1). In each patch, both species (species 1 and 2) and resource are present. We assume the asymmetric migration of species from one patch to another, i.e., the migration rates from patch-1 to patch-2 and conversely from patch-2 to patch-1 are not the same for each species. The local dynamics in each patch is governed by the Lotka-Volterra competition model (in the absence of migration). The dynamics of species in the presence of migration between two patches is given by the following equations:

$$\frac{dn_1^{(1)}}{dt} = \epsilon r_1 n_1^{(1)} \left(1 - \frac{n_1^{(1)}}{K} - \alpha_{12} \frac{n_2^{(1)}}{K} \right) + \left(-\bar{k} n_1^{(1)} + k n_1^{(2)} \right) , \qquad (4.1a)$$

$$\frac{dn_1^{(2)}}{dt} = \epsilon r_1 n_1^{(2)} \left(1 - \frac{n_1^{(2)}}{K} - \alpha_{12} \frac{n_2^{(2)}}{K} \right) + \left(\bar{k} n_1^{(1)} - k n_1^{(2)} \right) , \qquad (4.1b)$$

$$\frac{dn_2^{(1)}}{dt} = \epsilon r_2 n_2^{(1)} \left(1 - \alpha_{21} \frac{n_1^{(1)}}{K} - \frac{n_2^{(1)}}{K} \right) + \left(-\bar{m} n_2^{(1)} + m n_2^{(2)} \right) , \qquad (4.1c)$$

$$\frac{dn_2^{(2)}}{dt} = \epsilon r_2 n_2^{(2)} \left(1 - \alpha_{21} \frac{n_1^{(2)}}{K} - \frac{n_2^{(2)}}{K} \right) + \left(\bar{m} n_2^{(1)} - m n_2^{(2)} \right) , \qquad (4.1d)$$

where $n_1^{(1)}$ and $n_1^{(2)}$ represent the population densities of species 1 in patch-1 and patch-2, respectively. Similarly, $n_2^{(1)}$ and $n_2^{(2)}$, respectively, represent the population densities of species 2 in patch-1 and patch-2. The parameters \bar{k} and k represent migration rates of species 1 from patch-1 to patch-2 and from patch-2 to patch-1, respectively, while \bar{m} and m are the migration rates of species 2 from patch-1 to patch-2 and from patch-2 to patch-1, respectively. The parameter ϵ is a scaling factor that modulates the speed of population dynamics. This can be used to rescale the time as $t\epsilon \to t$, and similarly, the migration rates can be rescaled in the units of ϵ , and therefore, in what follows we will drop it for convenience. r_1 and r_2 are the intrinsic growth rates of species 1 and species 2, respectively. K is the carrying capacity of the environment, representing the

maximum population density that can be sustained in each patch. For simplicity, we are assuming that each patch has same carrying capacity, but for the case of different carrying capacities, one can do the following calculations along the same line. α_{12} is the competition coefficient indicating the effect of species 2 on species 1, while α_{21} indicates the effect of species 1 on species 2. For simplicity, we assume these competition coefficient to be patch independent.

4.3 Effective Asymmetric Migration model

We simplify the system by introducing two new variables that represent the total population densities of each species across the two patches: $n_1(t) \equiv n_1^{(1)}(t) + n_1^{(2)}(t)$ for species 1 and $n_2(t) \equiv n_2^{(1)}(t) + n_2^{(2)}(t)$ for species 2. These total densities, called global variables, stay constant when migration happens on a much faster time scale compared to local processes like growth and competition. Notice that the migration only redistributes species' individuals between the patches but does not change their overall numbers.

When migration is fast, the populations in each patch quickly settle into stable proportions, even though the total densities n_1 and n_2 remain fixed. In this case, the first term can be considered to be vanishingly small in each of the Eq. (4.1). To find these stable proportions, we assume that n_1 and n_2 are constant and calculate the stationary states of the migration terms using Eq. (4.1). For species 1, we obtain

$$n_1^{(1),*} = \frac{k}{k + \bar{k}} n_1 \equiv \theta_1^* n_1 ,$$

$$n_1^{(2),*} = \frac{\bar{k}}{k + \bar{k}} n_1 \equiv \theta_2^* n_1 ,$$

$$(4.2)$$

and for species 2, we have

$$n_2^{(1),*} = \frac{m}{m + \bar{m}} n_2 \equiv \mu_1^* n_2 ,$$

$$n_2^{(2),*} = \frac{\bar{m}}{m + \bar{m}} n_2 \equiv \mu_2^* n_2 ,$$
(4.3)

where the constants θ_1^* and θ_2^* represent the fast equilibrium proportions of species 1 in patch-1 and patch-2, respectively, while μ_1^* and μ_2^* represent the fast equilibrium proportions of species 2 in patch-1 and patch-2, respectively.

Now, returning to the complete model in Eq. (4.1), we express the system in terms of n_1 and n_2 . To write the equations in terms of n_1 and n_2 , we sum Eqs. (4.1a) and (4.1b), and Eqs. (4.1c) and (4.1d) of the full system (4.1). This results in

$$\frac{dn_1}{dt} = r_1 n_1 - \frac{r_1}{K} ([n_1^{(1)}]^2 + [n_1^{(2)}]^2) - \frac{\alpha_{12} r_1}{K} (n_1^{(1)} n_2^{(1)} + n_1^{(2)} n_2^{(2)}) , \qquad (4.4)$$

and similarly:

$$\frac{dn_2}{dt} = r_2 n_2 - \frac{r_2}{K} ([n_2^{(1)}]^2 + [n_2^{(2)}]^2) - \frac{\alpha_{21} r_2}{K} (n_1^{(1)} n_2^{(1)} + n_1^{(2)} n_2^{(2)}) . \tag{4.5}$$

Substituting the fast equilibria from equations (4.2) and (4.3)

$$n_1^{(1)} = \theta_1^* n_1 , \qquad (4.6a)$$

$$n_2^{(1)} = \mu_1^* n_2 ,$$
 (4.6c)

$$n_2^{(2)} = \mu_2^* n_2 ,$$
 (4.6d)

(these values of $n_1^{(1)},\ n_1^{(2)},\ n_2^{(1)}$ and $n_2^{(2)}$ are not at their stationary state values. The

stationary state values are given in Eqs. (4.2) and (4.3)) in Eqs. (4.4) and (4.5), we obtain leads to the following governing dynamical equations for species' population n_1 and n_2 :

$$\frac{dn_1}{dt} = r_1 n_1 \left(1 - \frac{(\theta_1^*)^2 + (\theta_2^*)^2}{K} n_1 - \alpha_{12} \frac{\theta_1^* \mu_1^* + \theta_2^* \mu_2^*}{K} n_2 \right) ,$$

$$\frac{dn_2}{dt} = r_2 n_2 \left(1 - \alpha_{21} \frac{\theta_1^* \mu_1^* + \theta_2^* \mu_2^*}{K} n_1 - \frac{(\mu_1^*)^2 + (\mu_2^*)^2}{K} n_2 \right) .$$
(4.7)

Further, by redefining $N_1 \equiv \frac{(\theta_1^*)^2 + (\theta_2^*)^2}{K} n_1$ and $N_2 \equiv \frac{(\mu_1^*)^2 + (\mu_2^*)^2}{K} n_2$, we obtain the effective dynamical equations for the species' population when species are migrating among two patches:

$$\frac{dN_1}{dt} = r_1 N_1 (1 - N_1 - a_{12} N_2) , \qquad (4.8)$$

$$\frac{dN_2}{dt} = r_2 N_2 (1 - a_{21} N_1 - N_2) , \qquad (4.9)$$

where we also redefine the competing stength as

$$a_{12} \equiv \alpha_{12} \frac{\theta_1^* \mu_1^* + \theta_2^* \mu_2^*}{(\mu_1^*)^2 + (\mu_2^*)^2} , \qquad (4.10)$$

$$a_{21} \equiv \alpha_{21} \frac{\theta_1^* \mu_1^* + \theta_2^* \mu_2^*}{(\theta_1^*)^2 + (\theta_2^*)^2} \ . \tag{4.11}$$

 N_1 and N_2 represent the scaled total population densities of species 1 and species 2, respectively. a_{12} indicates how strongly species 2 competes with species 1, relative to their resource needs, while a_{21} describes how strongly species 1 competes with species 2, relative to their resource utilization patterns.

Species coexistence: Stationary state and stabil-4.4 ity analysis

insight into potential ecological scenarios such as coexistence, dominance, or extinction of species. This subsection explores two key aspects of stationary states: their existence, determined by the interplay of migration rates and competitive interactions, and their stability, assessed by their resilience to small perturbations or tendency to shift under changing conditions. This analysis complements the broader mechanisms discussed earlier, enhancing our understanding of how asymmetric migration and competition shape the system's behavior.

4.4.1Stationary states of the system

Stationary states correspond to the points in the system where population densities no longer change over time. These are also called the *critical* or the *fixed* points. Henceforth, we label the critical point by 'CP'. For the asymmetric migration-competition model, the CPs are obtained when the rate of change of the population densities is zero. This implies solving the system of differential equations [Eqs. (4.8) and (4.9)]

$$\frac{dN_1}{dt} = r_1 N_1 \left(1 - N_1 - a_{12} N_2 \right) = 0 , \qquad (4.12)$$

$$\frac{dN_1}{dt} = r_1 N_1 (1 - N_1 - a_{12} N_2) = 0 ,$$

$$\frac{dN_2}{dt} = r_2 N_2 (1 - a_{21} N_1 - N_2) = 0 ,$$
(4.12)

simultaneously for N_1^* and N_2^* . Then, we obtain four critical points in the (N_1^*, N_2^*) plane: 1) CP1 \equiv (0,0), 2) CP2 \equiv (0,1), 3) CP3 \equiv (1,0), and 4) CP4 \equiv $\left(\frac{1-a_{12}}{1-a_{12}a_{21}}, \frac{1-a_{21}}{1-a_{12}a_{21}}\right)$

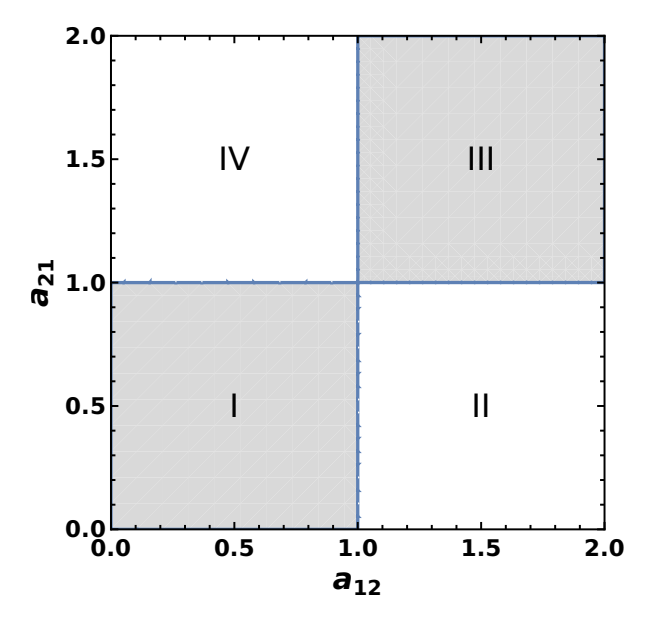


Figure 4.2: Plot illustrating the conditions for positive population densities of two species based on interaction coefficients a_{12} and a_{21} . The shaded region represents scenarios where both species have population densities greater than zero. In contrast, the unshaded regions show conditions where only one species maintains a positive population density.

The first critical point, CP1=(0,0), represents both species going extinct, which, though mathematically valid, is typically a rare scenario unless driven by external factors.

The second critical point, CP2=(0,1), occurs when species 1 goes extinct while species 2 persists at a density of 1. This reflects a situation where migration or competition favors the survival of species 2 over species 1. Conversely, the critical point CP3=(1,0) represents species 2's extinction and the persistence of species 1, occurring when species 1 outcompetes species 2 or benefits more from migration.

The fourth critical point CP4 corresponds to coexistence, where both species maintain positive, non-zero population densities, which imposes constraints on the competition coefficients a_{12} and a_{21} for this state to be feasible.

Together, these stationary states offer insight into possible long-term outcomes for the system. While the extinction states (0,0), (0,1), and (1,0) suggest scenarios where one or both species fail to persist, the coexistence state CP4 represents a balanced scenario where both species survive.

The phase diagram in Fig. 4.2 illustrates the relationship between the interaction coefficients a_{12} and a_{21} and the population dynamics of two competing species. The plot divides the parameter space into regions where different stationary states (critical points) occur. The shaded region represents the conditions where both species can coexist, maintaining positive population densities at stationary state, corresponding to critical point CP4. In contrast, the unshaded regions correspond to conditions where one species outcompetes the other, leading to competitive exclusion and the extinction of one species, as seen at critical points CP2 and CP3. The diagram visually summarizes the stability of these different outcomes based on the interaction coefficients, guiding predictions about the system's long-term behavior.

In the following analysis, we will assess the stability of these stationary states to determine which outcomes are more likely to occur under typical system conditions.

4.4.2 Stability analysis

The stability of stationary states (or critical points, CP) is critical for determining whether the system will return to these states after small perturbations or diverge toward alternative outcomes. Stability is analyzed using a Jacobian matrix [39], which is a matrix of partial derivatives that describes the dynamics of the system for small deviations around a given $CP=(x^*, y^*)$. For a system with two variables, the Jacobian

matrix is given by:

$$J = \begin{pmatrix} \frac{\partial f_1}{\partial x} & \frac{\partial f_1}{\partial y} \\ \frac{\partial f_2}{\partial x} & \frac{\partial f_2}{\partial y} \end{pmatrix} \Big|_{x^*, y^*} , \tag{4.14}$$

where $f_1(x, y)$ and $f_2(x, y)$ represent the system's governing functions, and x and y are the variables describing the system's state. The eigenvalues of the Jacobian matrix dictate stability: if both eigenvalues have negative real parts, the state is stable, and the system will return to it after perturbations. If both eigenvalues have positive real parts, the state is unstable, and the system will move away from it. States where one eigenvalue is positive and the other is negative are termed saddle points, which are stable along one direction but unstable along other (see Chapter 6 in Ref. [39] for more details on this topic).

For the extinction state CP1=(0,0), where both species are absent, the eigenvalues (λ_1, λ_2) of the Jacobian matrix are the intrinsic growth rates r_1 and r_2 of the species. Since these growth rates are typically positive, the extinction state is unstable, and small perturbations in population densities lead to population growth and movement away from this state.

For the single-species dominance states (0,1) and (1,0), stability depends on the competition coefficients. At (0,1), where species 2 persists at its carrying capacity and species 1 is extinct, the eigenvalues are $-r_2$ and $r_1(1-a_{12})$. If $a_{12} > 1$, species 2 strongly outcompetes species 1, and the state is stable. Conversely, if $a_{12} < 1$, the state becomes a saddle point. Similarly, at (1,0), where species 1 persists and species 2 is extinct, stability depends on the eigenvalues $-r_1$ and $r_2(1-a_{21})$. If $a_{21} > 1$, species 1 outcompetes species 2, resulting in stability, whereas $a_{21} < 1$ renders the state a saddle point.

The coexistence stationary state, $\left(\frac{1-a_{12}}{1-a_{12}a_{21}}, \frac{1-a_{21}}{1-a_{12}a_{21}}\right)$, represents a scenario where

both species persist at non-zero population densities. However, the eigenvalues of the Jacobian matrix for this state are cumbersome, making direct analysis of their signs challenging. To determine stability, we examine the sum and product of the eigenvalues. The sum of the eigenvalues is:

$$\lambda_1 + \lambda_2 = \frac{r_1(1 - a_{12}) + r_2(1 - a_{21})}{-1 + a_{12}a_{21}} , \qquad (4.15)$$

and the product is:

$$\lambda_1 \lambda_2 = -\frac{(-1 + a_{12})(-1 + a_{21})r_1 r_2}{-1 + a_{12}a_{21}} . \tag{4.16}$$

For the coexistence state to be stable, the sum of the eigenvalues must be negative as well as the product should be positive. These conditions depend on the interplay of competition coefficients (a_{12} and a_{21}) and growth rates (r_1 and r_2). If either of the conditions on the sum and products of eigenvalues is violated, the coexistence state is not stable fixed point, reflecting mixed stability properties. These conditions highlight the delicate balance required for coexistence and underscore the sensitivity of this state to changes in growth rates and competition coefficients. To check the stability of CP4 in the regions where $0 < a_{12} < 1$ and $0 < a_{21} < 1$ and $a_{12} > 1$ and $a_{21} > 1$, we analyze the sum (4.15) and product (4.16) of the eigenvalues.

In the first case, where $0 < a_{12} < 1$ and $0 < a_{21} < 1$, we check the sum of the eigenvalues (4.15). Since both $1 - a_{12}$ and $1 - a_{21}$ are positive and the $-1 + a_{12}a_{21}$ is also positive, the sum of the eigenvalues is negative, satisfying the condition for stability. Additionally, when we check the product (4.16), it will be positive, as the terms in the numerator and denominator remain positive. This indicates that CP4 is stable in this region.

In the second case, where both $a_{12} > 1$ and $a_{21} > 1$, we check the product of the

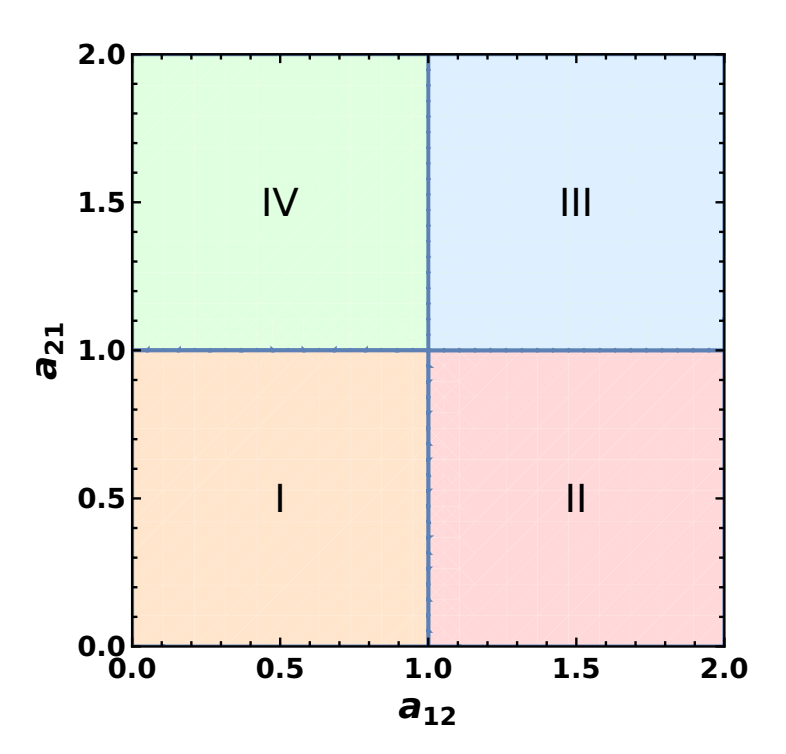


Figure 4.3: Stability regions for critical points (CPs) in the parameter space of a_{12} and a_{21} . The plot is divided into four regions: region I (light orange) where CP4 is stable, region II (light pink) where CP2 is stable, region III (light blue) where both CP2 and CP3 are stable, and region IV (light green) where CP3 is stable.

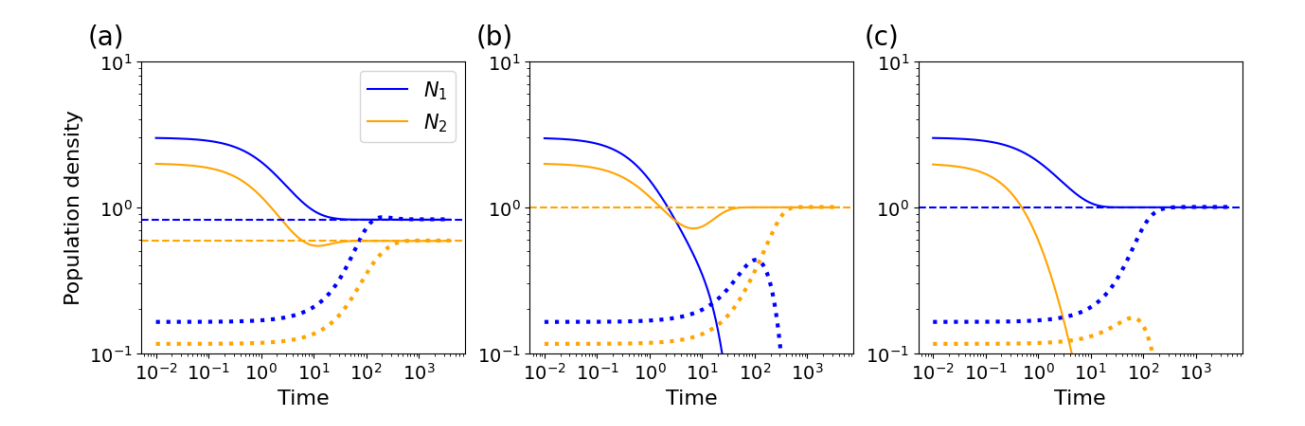


Figure 4.4: Time evolution of scaled population densities of species 1 (blue) and species 2 (orange) under different interaction scenarios. In this plot, outcomes from the original system (Eq. (4.1)) are shown with dotted lines, the results from the simplified (Eqs. (4.8) and (4.9)) are represented by solid lines, and the analytical results are indicated by dashed lines. Panel a represents the case where $0 < a_{12} < 1$ and $0 < a_{21} < 1$. Panel b corresponds to the scenario where $a_{12} > 1$ and $0 < a_{21} < 1$. Finally, panel c depicts the case where $0 < a_{12} < 1$ and $a_{21} > 1$. The parameters used are $a_{11} = 0.2$ and $a_{21} = 0.3$, representing the growth rates of species 1 and 2, respectively. The migration rates of species 1 are $a_{12} = 0.3$ (from patch-2 to patch-1) and $a_{12} = 0.3$ (from patch-1 to patch-2), while the migration rates of species 2 are $a_{12} = 0.3$ (from patch-2 to patch-1) and $a_{12} = 0.3$ (from patch-1 to patch-2). The scaling factor $a_{12} = 0.3$ (from patch-1 to patch-2). The scaling factor $a_{13} = 0.3$ (from patch-1 to patch-2). The scaling factor $a_{13} = 0.3$ (from patch-1 to patch-2), and the carrying capacity is $a_{13} = 0.3$ (from patch-2) and $a_{13} = 0.3$ (from patch-2), and the carrying capacity is $a_{13} = 0.3$ (from patch-2) and $a_{13} = 0.3$ (from patch-2) and $a_{14} = 0.3$ (from patch-2) and (4.8) and (4.9), and Eqs. (4.1a), (4.1b), (4.1c) and (4.1d) were solved via numerical integration using Euler's method (see Appendix 6).

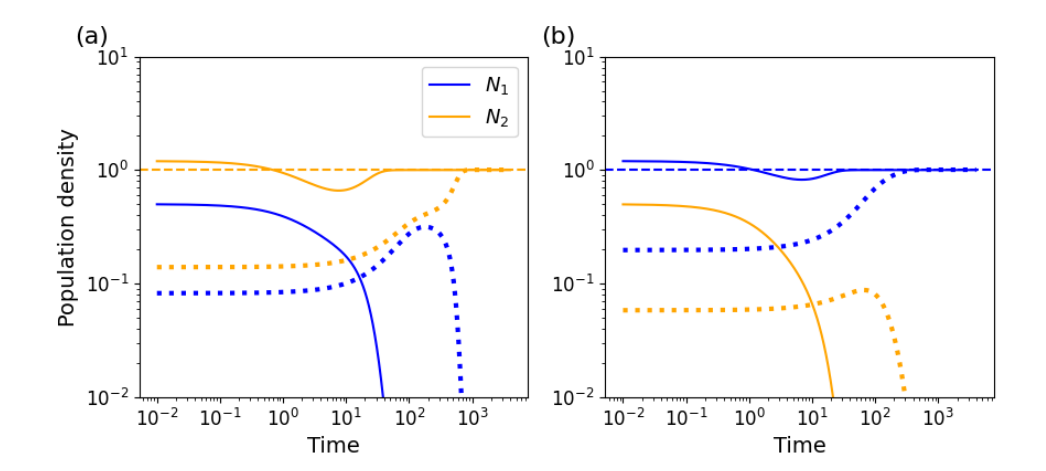


Figure 4.5: Time evolution of scaled population densities of species 1 (blue) and species 2 (orange) for the case where $a_{12} > 1$ and $a_{21} > 1$ ($a_{12} = 1.7$, $a_{21} = 1.7$). In this plot, outcomes from the original system (Eq. (4.1)) are shown with dotted lines, the results from the simplified (Eqs. (4.8) and (4.9)) are represented by solid lines, and the analytical results are indicated by dashed lines. Panel a represents the dynamics with initial population densities $N_1 = 0.5$ and $N_2 = 1.2$. Panel b shows the dynamics with initial population densities $N_1 = 1.2$ and $N_2 = 0.5$. The parameters used are $r_1 = 0.2$ and $r_2 = 0.3$, representing the growth rates of species 1 and 2, respectively. The migration rates of species 1 are k = 0.9 (from patch-2 to patch-1) and $\bar{k} = 0.1$ (from patch-1 to patch-2), while the migration rates of species 2 are m = 0.7 (from patch-2 to patch-1) and $\bar{m} = 0.3$ (from patch-1 to patch-2). The scaling factor $\epsilon = 0.1$ modulates the speed of population dynamics, and the carrying capacity is K = 5. The interaction coefficients a_{12} and a_{21} represent the effects of species 2 on species 1 and species 1 on species 2. The dynamics [Eqs. (4.8) and (4.9), and Eqs. (4.1a), (4.1b), (4.1c) and (4.1d)] were solved via numerical integration using Euler's method (see Appendix 6).

eigenvalues (Eq. (4.16)), we find that it is negative because both $-1 + a_{12}$ and $-1 + a_{21}$ are positive and $-1 + a_{12}a_{21}$ is also positive, violating the stability condition that the product must be positive. This shows that CP4 is unstable in this region.

In conclusion, CP4 is stable in the region where $0 < a_{12} < 1$ and $0 < a_{21} < 1$, but it is unstable in the region where $a_{12} > 1$ and $a_{21} > 1$.

Figure 4.3 shows how the stability of the critical points (CPs) affects the survival of the species. In region I, where CP4 is stable, both species survive and coexist. In region II, where CP2 is stable, species 2 survives while species 1 goes extinct. In region III, both CP2 and CP3 are stable, meaning one species will survive and the other will die, depending on the initial conditions. In region IV, where CP3 is stable, species 1 survives and species 2 dies. The stability of these critical points does not depend on the values of r_1 and r_2 , but only on the values of a_{12} and a_{21} . This shows that the stability of the CPs is determined by these parameters alone.

Figure 4.4 demonstrates that when both a_{12} and a_{21} are greater than zero but less than one, both species coexist (panel a). When a_{12} exceeds one and a_{21} is greater than zero but less than one, species 2 survives while species 1 extinct (panel b). Conversely, when a_{12} is greater than zero but less than one and a_{21} exceeds one, species 1 survives while species 2 goes extinct (panel c). These outcomes align with the predictions made in Fig. 4.3 regarding the stability of different critical points for varying values of a_{12} and a_{21} .

Figure 4.5 demonstrates that changing the initial conditions (initial population densities of species) while keeping the interspecific interaction coefficients constant leads to different outcomes, highlighting the bistable nature of the system. In panel a, species 2 survives while species 1 goes extinct, and in panel b, species 1 survives while species

2 goes extinct. This supports the result discussed in Fig. 4.3, where high values of the interspecific interaction coefficients lead to two stationary states, (1,0) and (0,1)

In Figs. 4.4 and 4.5 we also numerically simulated the full dynamics (4.1) and compared with the effective dynamics (4.8) and (4.9), we found an excellent agreement in the long-time limit, as expected.

4.4.3 Coexistence condition in terms of original competition coefficients (α_{12} and α_{21})

From Eqs. (4.10) and (4.11), we have the relationships between the rescaled competition coefficients (a_{12} and a_{21}) and the original competition coefficients (α_{12} and α_{21}). Using these relationships and the coexistence condition derived from Fig. 4.3, we can express the coexistence condition directly in terms of α_{12} and α_{21} .

As defined earlier in Eqs. (4.10) and (4.11), a_{12} and a_{21} depend on α_{12} , α_{21} , and the dimensionless parameters. For coexistence, the condition $a_{12} < 1$ and $a_{21} < 1$ must hold.

Substituting the expressions for a_{12} and a_{21} into the coexistence condition, we rewrite it in terms of α_{12} and α_{21} :

$$\alpha_{12} \frac{(1+\phi_m)(1+\phi_m\phi_k)}{(1+\phi_k)(1+\phi_m^2)} < 1, \tag{4.17}$$

$$\alpha_{21} \frac{(1+\phi_k)(1+\phi_m\phi_k)}{(1+\phi_m)(1+\phi_k^2)} < 1, \tag{4.18}$$

where $\phi_k = \frac{k}{\bar{k}}$ and $\phi_m = \frac{m}{\bar{m}}$ are dimensionless quantities, with k, \bar{k}, m and \bar{m} representing migration rates as defined earlier.

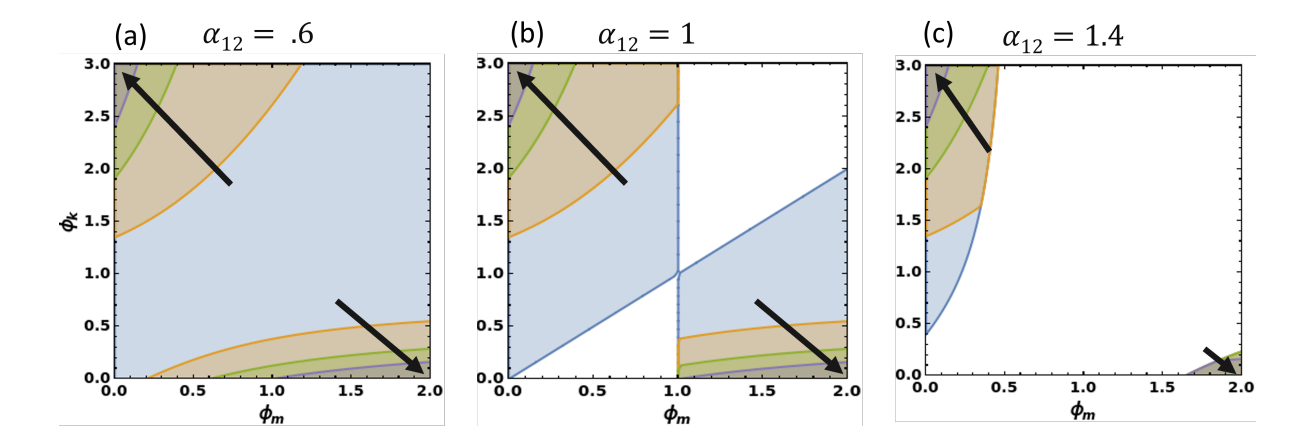


Figure 4.6: Coexistence regions in the ϕ_m and ϕ_k parameter space for different values of the original competition coefficient α_{12} ($\alpha_{12} = 0.6, 1.0, \text{ and } 1.4$). The shaded regions indicate where coexistence occurs. The black arrows show the direction of increasing α_{21} , illustrating how coexistence conditions change with its variation.

Figure 4.6 demonstrates how changes in α_{12} and α_{21} influence the coexistence regions in the ϕ_m and ϕ_k parameter space. Each panel corresponds to a different value of α_{12} , while the colored regions within each panel represent the coexistence for different values of α_{21} , where α_{21} increases in the direction of the black arrow.

As the values of α_{12} and α_{21} increase, the coexistence region decreases. This result aligns with theoretical expectations: increasing α_{12} and α_{21} reflects intensifying competition between species. When competition outweighs migration, coexistence becomes less feasible. Thus, these plots illustrate the critical interplay between competition and migration in determining the conditions for coexistence.

4.5 Conclusion

In this chapter, we showed that asymmetric migration can promote species coexistence in competitive environments. Migration alters the effective competition coefficients and enables species to persist even when classical CEP models predict exclusion. Our analytical results and simulations illustrate how spatial coupling expands the range of coexistence.

Having now examined ecological stability from statistical, mechanistic, and spatial perspectives, we conclude this thesis with an *Outlook* chapter. There, we reflect on the broader significance of these findings and suggest directions for future theoretical and empirical research.

Chapter 5

Summary and outlook

Understanding the stability and coexistence of species in ecological systems remains one of the most fundamental challenges in theoretical ecology. In this thesis, we approached this problem from three distinct yet interconnected perspectives: spectral stability in large ecosystems, mechanistic competition via consumer-resource dynamics, and migration-enabled coexistence in spatially structured systems.

Our exploration began with random matrix theory, where we revisited May's stability criterion and extended it using tools like the Circular Law, sparsity, and variance rescaling. These results provided system-level insights into how complexity affects stability and highlighted the power of statistical methods for analyzing high-dimensional ecological networks.

We then transitioned to a species-centric perspective using consumer-resource models. Here, we revisited the classical competitive exclusion principle and examined how species traits and resource supply conditions determine coexistence or exclusion. Using geometric tools such as Zero Net Growth Isoclines (ZNGIs), we developed intuition for how niche overlap and resource availability influence ecological outcomes.

Finally, we introduced spatial structure and studied how asymmetric migration between habitat patches reshapes effective competition. Migration not only weakens local exclusionary dynamics but also creates opportunities for species to persist across landscapes. This spatial perspective enriches our understanding of biodiversity maintenance in fragmented or heterogeneous environments.

Future Directions

While the models and results presented here offer valuable insights, they also open up several directions for future research:

- Beyond two patches: Extending the migration model to multiple patches or networked landscapes could capture richer spatial dynamics, including source-sink effects and metacommunity structure [40, 41, 42].
- **Temporal variability:** Incorporating time-varying resource supply or migration rates would allow exploration of how environmental fluctuations affect stability and coexistence [43, 44].
- Eco-evolutionary dynamics: Coupling ecological interactions with evolutionary change (e.g., in resource use traits or dispersal strategies) may reveal feedback loops that further shape biodiversity patterns [45, 46, 47].

- Empirical testing: It would be valuable to connect these theoretical predictions with data from real ecosystems, particularly microbial communities or island networks where migration and competition are both observable [48, 49, 50].
- Interdisciplinary extensions: The frameworks developed here—especially the spectral and dynamical systems approaches—may also be applied to other complex systems, such as social, technological, or economic networks where stability and persistence are of interest [51, 52, 53].

In sum, this thesis contributes to a deeper understanding of how species persist in competitive environments and how complexity, structure, and movement shape ecological outcomes. We hope that the perspectives developed here will serve as a foundation for further theoretical development and real-world application.

Chapter 6

APPENDIX

In this appendix, we describe Euler's method, a basic numerical technique for approximating solutions to ordinary differential equations [54]. This method is employed in the numerical simulations throughout the thesis. Specifically, for all figures and results involving the time evolution of differential equation-particularly those derived from our dynamical system models—Euler's method was used to compute approximate solutions. This chapter outlines the mathematical basis of the method and includes an analysis of its numerical error.

6.1 Euler's Method

Euler's method is a simple numerical technique used to approximate the solution of a first-order differential equation of the form:

$$\frac{dy}{dx} = f(x, y), \quad y(x_0) = y_0.$$
 (6.1)

The goal is to estimate the values of y at discrete points $x = x_r = x_0 + rh$ for $r = 1, 2, 3, \ldots$, where h is a small step size.

To derive Euler's formula, we integrate both sides of the differential equation from x_0 to $x_1 = x_0 + h$:

$$y_1 = y_0 + \int_{x_0}^{x_1} f(x, y) \, dx . \tag{6.2}$$

If we assume that f(x, y) remains approximately constant over this small interval and take its value at (x_0, y_0) , we obtain the following approximation:

$$y_1 \approx y_0 + hf(x_0, y_0)$$
 (6.3)

Similarly, for the next step from x_1 to x_2 , integrating the differential equation gives:

$$y_2 = y_1 + \int_{x_1}^{x_2} f(x, y) \, dx . \tag{6.4}$$

Approximating f(x,y) by its value at (x_1,y_1) results in:

$$y_2 \approx y_1 + h f(x_1, y_1)$$
 (6.5)

By continuing this process, we derive the general formula for Euler's method:

$$y_{n+1} = y_n + hf(x_n, y_n), \quad n = 0, 1, 2, \dots$$
 (6.6)

6.1.1 Error Analysis in Euler's Method

Euler's method introduces numerical errors because it assumes that f(x, y) remains constant over each step. To analyze the error, we derive the local truncation error and the global error.

Local Truncation Error

Using Taylor series expansion, the exact solution at $x_{n+1} = x_n + h$ is:

$$y(x_{n+1}) = y(x_n) + hy'(x_n) + \frac{h^2}{2}y''(x_n) + \frac{h^3}{6}y'''(x_n) + O(h^4) . \tag{6.7}$$

Since $y'(x_n) = f(x_n, y_n)$, substituting this in the expansion gives:

$$y(x_{n+1}) = y_n + hf(x_n, y_n) + \frac{h^2}{2}y''(x_n) + O(h^3) .$$
 (6.8)

Comparing this with Euler's approximation:

$$y_{n+1}^{\text{(Euler)}} = y_n + h f(x_n, y_n) ,$$
 (6.9)

we find that the local truncation error at each step is:

$$E_{\text{local}} = y(x_{n+1}) - y_{n+1}^{(\text{Euler})} = \frac{h^2}{2}y''(x_n) + O(h^3).$$
 (6.10)

Thus, the local error is proportional to h^2 , meaning that for small h, the error at each step is approximately $O(h^2)$.

Global Error

The global error is the accumulation of local errors over multiple steps. Suppose we approximate the solution over an interval from x_0 to x_N , using N steps of size h, where $N = \frac{x_N - x_0}{h}$.

Since the local error at each step is $O(h^2)$, the total error after N steps is:

$$E_{\text{global}} = N \cdot O(h^2) \ . \tag{6.11}$$

Substituting $N = \frac{x_N - x_0}{h}$:

$$E_{\text{global}} = \frac{x_N - x_0}{h} \cdot O(h^2) . \tag{6.12}$$

Simplifying,

$$E_{\text{global}} = O(h). \tag{6.13}$$

This result shows that Euler's method has a global error of order O(h), meaning the overall error decreases linearly as $h \to 0$. However, this also implies that for better accuracy, we need a very small step size, which increases computational effort.

Bibliography

- [1] Michel et al. Loreau. Biodiversity and ecosystem functioning: current knowledge and future challenges. *Science*, 294(5543):804–808, 2001.
- [2] David U. et al. Hooper. Effects of biodiversity on ecosystem functioning: a consensus of current knowledge. *Ecological Monographs*, 75(1):3–35, 2005.
- [3] Bradley J. et al. Cardinale. Biodiversity loss and its impact on humanity. *Nature*, 486:59–67, 2012.
- [4] Alfred J. Lotka. Elements of Physical Biology. Williams and Wilkins, 1925.
- [5] Vito Volterra. Fluctuations in the abundance of a species considered mathematically. Nature, 118:558–560, 1926.
- [6] Simon A. Levin. Ecosystems and the biosphere as complex adaptive systems. *Ecosystems*, 1(5):431–436, 1998.
- [7] Kevin S. McCann. The diversity-stability debate. Nature, 405:228–233, 2000.
- [8] Robert M. May. Will a large complex system be stable? *Nature*, 238:413–414, 1972.
- [9] Robert M. May. Stability and Complexity in Model Ecosystems. Princeton University Press, 1973.

- [10] Terence Tao and Van Vu. Random matrices: Universality of local eigenvalue statistics up to the edge. *Communications in Mathematical Physics*, 298(2):549–572, 2010.
- [11] Stefano Allesina and Si Tang. Stability criteria for complex ecosystems. *Nature*, 483:205–208, 2012.
- [12] Jacopo Grilli, György Barabás, Matthew J. Michalska-Smith, and Stefano Allesina. Higher-order interactions stabilize dynamics in competitive network models. *Nature*, 548(7666):210–213, 2017.
- [13] Giulio Biroli, Guy Bunin, and Chiara Cammarota. Marginally stable equilibria in critical ecosystems. *New Journal of Physics*, 20(8):083051, 2018.
- [14] Jean-François Arnoldi, Michel Loreau, and Bart Haegeman. Resilience, reactivity and variability: A mathematical comparison of ecological stability measures. *Jour*nal of Theoretical Biology, 389:47–59, 2016.
- [15] G. F. Gause. The Struggle for Existence. Williams and Wilkins, 1934.
- [16] Garrett Hardin. The competitive exclusion principle. *Science*, 131(3409):1292–1297, 1960.
- [17] Robert H. MacArthur. Species packing and competitive equilibrium for many species. *Theoretical Population Biology*, 1(1):1–11, 1970.
- [18] David Tilman. Resource Competition and Community Structure. Princeton University Press, 1982.
- [19] Peter Chesson. Mechanisms of maintenance of species diversity. *Annual Review of Ecology and Systematics*, 31:343–366, 2000.

- [20] Priyanga Amarasekare. Competitive coexistence in spatially structured environments: a synthesis. *Ecology Letters*, 6(12):1109–1122, 2003.
- [21] Robert D. Holt. Ecology at the mesoscale: the influence of regional processes on local communities. Species Diversity in Ecological Communities, pages 77–88, 1993.
- [22] Robert H. MacArthur. Fluctuations of animal populations and a measure of community stability. *Ecology*, 36(3):533–536, 1955.
- [23] M. R. Gardner and W. R. Ashby. Connectance of large dynamic (cybernetic) systems: critical values for stability. *Nature*, 228:784, 1970.
- [24] Guy Bunin. Ecological communities with lotka-volterra dynamics. *Phys. Rev. E*, 95:042414, 2017.
- [25] Zhidong D. Bai. Circular law. Annals of Probability, 25(1):494–529, 1997.
- [26] Terence Tao and Van Vu. Random matrices: universality of esds and the circular law. *The Annals of Probability*, 38(5):2023–2065, 2010.
- [27] Yan V. Fyodorov and Hans-Jürgen Sommers. Random matrices close to hermitian or unitary: overview of methods and results. *Journal of Physics A: Mathematical and Theoretical*, 40(25):F671–F700, 2007.
- [28] Tyler Gibbs, Jacopo Grilli, and Tim Rogers. Effect of population abundances on the stability of large random ecosystems. *Phys. Rev. E*, 98(2):022410, 2018.
- [29] A. Edelman. Eigenvalues and condition numbers of random matrices. SIAM Journal on Matrix Analysis and Applications, 9(4):543–560, 1988.
- [30] E. P. Wigner. Characteristic vectors of bordered matrices with infinite dimensions.

 Annals of Mathematics, 62(3):548–564, 1955.

- [31] J. Wishart. The generalised product moment distribution in samples from a normal multivariate population. *Biometrika*, 20A(1-2):32–52, 1928.
- [32] V. A. Marčenko and L. A. Pastur. Distribution of eigenvalues for some sets of random matrices. *Mathematics of the USSR-Sbornik*, 1(4):457–483, 1967.
- [33] A. Soshnikov. A note on universality of the distribution of the largest eigenvalues in certain sample covariance matrices. *Journal of Statistical Physics*, 108(5-6):1033– 1056, 2002.
- [34] G. Ben Arous and A. Guionnet. Wigner matrices. In Oxford Handbook of Random Matrix Theory. Oxford University Press, 2011.
- [35] J. P. Bouchaud and M. Potters. Theory of Financial Risk and Derivative Pricing: From Statistical Physics to Risk Management. Cambridge University Press, 2000.
- [36] Steven H Strogatz. Nonlinear Dynamics and Chaos: With Applications to Physics, Biology, Chemistry, and Engineering. CRC Press, 2018.
- [37] Alan Hastings. Can spatial variation alone lead to coexistence? Theoretical Population Biology, 24(3):244–251, 1983.
- [38] Priyanga Amarasekare. Spatial dynamics of foodwebs. Annual Review of Ecology, Evolution, and Systematics, 39:479–500, 2008.
- [39] Steven H. Strogatz. Nonlinear Dynamics and Chaos: With Applications to Physics, Biology, Chemistry, and Engineering. Westview Press, Boulder, CO, 2nd edition edition, 2015.
- [40] MA Leibold, M Holyoak, N Mouquet, et al. The metacommunity concept: a framework for multi-scale community ecology. *Ecology Letters*, 7:601–613, 2004.

- [41] M Holyoak, MA Leibold, and RD Holt. *Metacommunities: spatial dynamics and ecological communities*. University of Chicago Press, 2005.
- [42] D Gravel, N Mouquet, M Loreau, and F Guichard. Source and sink dynamics in meta-ecosystems. *Ecology Letters*, 14(7):723–732, 2011.
- [43] P Chesson. Multispecies competition in variable environments. *Theoretical Population Biology*, 45:227–276, 1994.
- [44] SP Ellner, RE Snyder, PB Adler, and G Hooker. How to quantify the temporal storage effect using simulations instead of math. *Ecology Letters*, 22:179–187, 2019.
- [45] TW Schoener. The newest synthesis: understanding the interplay of evolutionary and ecological dynamics. *Science*, 331:426–429, 2011.
- [46] MC Urban and L De Meester. A framework for incorporating evolutionary history into community ecology. *Ecology Letters*, 15(8):773–786, 2012.
- [47] T Fukami. Historical contingency in community assembly: integrating niches, species pools, and priority effects. Annual Review of Ecology, Evolution, and Systematics, 46:1–23, 2015.
- [48] S Estrela, A Sanchez-Gorostiaga, JCC Vila, et al. Metabolic rules of microbial community assembly. *Science*, 377:eabl8852, 2022.
- [49] DR Nemergut, SK Schmidt, T Fukami, et al. Patterns and processes of microbial community assembly. *Microbiology and Molecular Biology Reviews*, 77:342–356, 2013.

- [50] JB Logue, N Mouquet, H Peter, and H Hillebrand. Empirical approaches to metacommunities: a review and comparison with theory. Trends in Ecology Evolution, 26:482–491, 2011.
- [51] MEJ Newman. Networks: An Introduction. Oxford University Press, 2010.
- [52] J Gao, B Barzel, and AL Barabási. Universal resilience patterns in complex networks. *Nature*, 530:307–312, 2016.
- [53] Stefano Allesina and Si Tang. The stability-complexity relationship at age 40: a random matrix perspective. *Population Ecology*, 57(1):63–75, 2015.
- [54] Richard L. Burden and J. Douglas Faires. Numerical Analysis. Cengage Learning, 9th edition, 2011.